Journal of Analytical and Applied Pyrolysis 173 (2023) 106087

Contents lists available at ScienceDirect

Journal of Analytical and Applied Pyrolysis

journal homepage: www.elsevier.com/locate/jaap

Enhancing the pyrolytic conversion of biosolids to value-added products via mild acid pre-treatment

Ibrahim Gbolahan Hakeem [a,b], Pobitra Halder [b,c], Savankumar Patel [a,b], Abhishek Sharma [b,d], Rajender Gupta [e], Aravind Surapaneni [b,f], Jorge Paz-Ferreiro [a], Kalpit Shah [a,b,*]

[a] Chemical and Environmental Engineering, School of Engineering, RMIT University, Melbourne, VIC 3000, Australia
[b] ARC Training Centre for the Transformation of Australia's Biosolids Resources, RMIT University, Bundoora, VIC 3058, Australia
[c] School of Engineering, Deakin University, VIC 3216, Australia
[d] Department of Chemical Engineering, Manipal University Jaipur, Rajasthan 303007, India
[e] Department of Chemical & Materials Engineering, University of Alberta, Edmonton, Canada
[f] South East Water Corporation, Frankston, VIC 3199, Australia

ARTICLE INFO

Keywords:
Demineralisation
Metal passivation
Sewage sludge
Pyrolysis
Heavy metals

ABSTRACT

High concentrations of inorganic matter such as silicates, alkali and alkaline earth metals (AAEMs), and heavy metals (HMs) in biosolids limit their pyrolysis conversion to high-value products. Therefore, the reduction or passivation of the deleterious pyrolytic activities of these native inorganics in biosolids can enhance the yield and quality of products obtained during pyrolysis. The pyrolysis of raw and 3% sulfuric acid pre-treated biosolids was carried out in a fluidised bed reactor at 300–700 ℃, and the influence of pre-treatment was examined on biochar properties, gas production, and bio-oil composition. At all temperatures, the selective removal of ash-forming elements (demineralisation) in biosolids by pre-treatment improved organic matter devolatilisation yielding higher bio-oil and lower biochar than untreated biosolids. Demineralisation weakened gas production, particularly at higher pyrolysis temperatures. At 700 ℃, the in-situ formation of acidic metal sulfate salts in sulfuric acid-infused biosolids facilitated H^+ release, thereby increasing H_2 yield to a maximum of 15 mol% compared to 8 mol% from untreated biosolids and 4 mol% from demineralised biosolids. Biochar produced from treated biosolids had considerably lower HMs concentration and higher organic matter retention compared to raw biosolids biochar. The effect of pre-treatment on biochar properties was profound at 700 ℃ pyrolysis temperature. Pre-treatment increased biochar fixed carbon by 57%, calorific value by 37%, fuel ratio by 44%, doubled the specific surface area from 55 to 107 m^2/g, and enhanced porous structure formation. At 300 ℃, the major chemical compounds in the bio-oil were amides (20%), N-heterocyclics (25%), and ketones (30%), and higher temperatures favoured phenols and aromatic hydrocarbon production. Pre-treatment enhanced the selectivity of furans by 10-fold, anhydrosugars by 2-fold, and aromatic hydrocarbons by 1.5-fold relative to the raw biosolids bio-oil. Acid pre-treatment is a promising strategy for improving biosolids quality as feedstock for pyrolysis to generate high-value products.

1. Introduction

Biosolids (stabilised sewage sludge) are solid residues of the wastewater treatment process. Biosolids are enriched with plant nutrients (N, P, K), facilitating their widespread application on agricultural land. However, the presence of microbial, organic, and inorganic contaminants is reducing the attractiveness of biosolids for direct land application [1]. Therefore, a substantial volume of biosolids may not be safely applied on land due to increasingly stringent regulations on biosolids management. Non-combustive thermal techniques such as pyrolysis, gasification, and hydrothermal carbonisation/liquefaction have been widely demonstrated for treating biosolids with the potential for contaminant destruction and resource recovery [2,3]. Pyrolysis is the most promising thermal treatment technique for biosolids processing and has been extensively studied under different conditions. At typical pyrolysis conditions (usually 400–700 °C under an inert atmosphere), pathogens and organic contaminants can be effectively degraded, and the waste volume can be reduced by at least 30% while generating solid

* Corresponding author at: Chemical and Environmental Engineering, School of Engineering, RMIT University, Melbourne, VIC 3000, Australia.
E-mail addresses: ibrahim.hakeem@rmit.edu.au (I.G. Hakeem), kalpit.shah@rmit.edu.au (K. Shah).

https://doi.org/10.1016/j.jaap.2023.106087
Received 17 May 2023; Received in revised form 13 July 2023; Accepted 15 July 2023
Available online 18 July 2023

(biochar), liquid (bio-oil), and gaseous (syngas) products [4]. However, despite these promising outcomes, biosolids pyrolysis can be limited by low conversion, poor selectivity, and product contamination [5]. Unlike lignocellulosic biomass, biosolids can have high amounts of inorganic matter (up to 50 wt%), depending on the source and stabilisation method [6]. The high ash content (and low volatile solids) may limit the suitability of biosolids as a pyrolysis feedstock. The inorganic content such as silicates, aluminates, alkali and alkaline earth minerals (AAEMs), and heavy metals (HMs) can inhibit the conversion of organic matter and interferes with the formation pathway of valuable chemical compounds during pyrolysis [7]. After pyrolysis, the inorganic minerals are largely retained in the biosolids-derived biochar at a higher concentration with deleterious influence on the biochar physicochemical properties and application potential [8]. For example, biosolids biochar with higher HMs concentration may not be attractive for land application. Excessively high amounts of ash content and inorganic minerals in biochar can reduce the oxidation resistance of the biochar carbon, lower the ash fusion temperature, and induce slagging and fouling during combustion for energy recovery [9]. Also, higher concentrations of minerals can lower chars' activation potential, reduce microporous structure development, and decrease the specific surface areas [10].

Three improvement strategies, such as i) feed pre-treatment, ii) use of catalysts, and iii) feed co-processing, have been demonstrated to enhance the pyrolytic conversion of biosolids to high-value products [11]. The extensively studied approaches are co-pyrolysis and in-situ catalytic pyrolysis, which involves the wet or dry mixing of biosolids with other biomass feedstock or catalyst additives [12–14]. Besides the opportunity to manage more than one waste stream, the potential advantages of co-processing biosolids with other feedstock in the presence or absence of catalysts include improved process selectivity, faster conversion kinetics, suppression of pollutant release, and enhanced product properties [15,16]. Co-pyrolysis, catalytic pyrolysis, and their combinations have been demonstrated to improve the pyrolytic conversion of biosolids through beneficial synergistic interactions of co-feedstock and catalysts additive. However, there are still some technical issues that require further attention, such as (i) deconvolution of the complex conversion kinetics and synergistic interactions, (ii) poor product homogeneity arising from feedstock variability and feed particle segregation, and (iii) difficulty in catalyst separation and recovery during in-situ operations.

The chemical pre-treatment of biosolids as an initial process step before pyrolysis has not been fully explored. Previous works suggested that mild acid pre-treatment of biosolids can selectively remove inorganic elements and partially hydrolyse recalcitrant organics to produce organic-rich residue suitable for pyrolysis conversion to bio-oil [8,17–19]. During acid pre-treatment, protons (H^+) from the acid solution replaced free or loosely bound metal ions in biosolids via an ion exchange mechanism, causing the removal of ash-forming elements [11]. Also, deprotonation of carboxylic O–H and hydroxylic O–H functional groups can produce many H^+ and negatively charged polyions that promote the desorption of metal ions in biosolids [20]. Depending on the severity of the acid pre-treatment conditions, disintegration (hydrolysis) of organic matter in biosolids can occur attributed to the disruption of hydroxyl bonds and cleavage of carbonyl groups, as well as the transformation of crystalline compounds to amorphous form, thereby reducing the structural and thermal recalcitrance of the treated residue [21,22]. For example, mild acid (<5% H_2SO_4 at 25 ℃ and 1 h) pre-treatment of biosolids was reported to remove about 75–95% of inherent HMs and 80–95% AAEMs, which reduced the ash content by 50% without degradation of organic constituents [17]. Then, the pyrolysis of acid-pre-treated biosolids had higher rates of devolatilisation occurring at lower temperatures to produce lower char residues than untreated biosolids [8,17]. Similarly, Liu et al. [18] reported that acid washing using 0.1 M H_2SO_4 at ambient conditions for 12 h reduced biosolids ash content from 32 wt% to 20 wt% and increased carbon content by 26%. Therefore, acid pre-treatment of biosolids before pyrolysis may be desired for many reasons, such as (i) reduction of HMs concentration and bioavailability in the resultant biochar, (ii) reduction of ash content and increased organic matter retention in biochar, (iii) enhancement of char textural properties and specific surface area, and (iv) improvement of both energy and chemical value of bio-oil through reduction of water and oxygenates content ordinarily catalysed by native AAEMs. Furthermore, there is an extensive demonstration of acid pre-treatment of biosolids for removing HMs and other limiting contaminants, thereby improving the grade of biosolids for unrestricted beneficial land reuse [20,23,24]. Therefore, biosolids pre-treatment may have a two-fold benefit for improving biosolids quality for land application as well as for pyrolysis upcycling.

Existing studies on integrated acid pre-treatment and pyrolysis were centred on understanding the role of inherent metals on biosolids' thermal decomposition behaviour and pyrolysis kinetics [19,25,26]. The analytical pyrolysis of acid-demineralised biosolids or demineralised biosolids spiked with specific metal additive have been used to elucidate the catalytic role of internal or added metals in fostering or inhibiting the release of gaseous nitrogen and sulfur compounds, degradation characteristics of organic matter, volatiles evolution, and pyrolysis activation energy [19,25–27]. There are limited studies on the bench-scale pyrolysis of acid-treated biosolids [18,28]. The role of acid pre-treatment on the distribution of pyrolysis product fractions (oil, char, and gas) and their properties have not been fully documented in the literature. Also, the observed effect of pre-treatment of biosolids in analytical pyrolysis setup may differ in practical reactor systems such as the fluidised bed reactor where gas-solid interactions are faster due to improved mass and heat transfer. Hence, biosolids pre-treatment before pyrolysis demands an extensive investigation in a typical fluid bed reactor under wide conditions of pre-treatment and pyrolysis.

This work studied the pyrolysis of raw and acid-treated biosolids in a fluidised bed reactor at 300–700 ℃ to understand the role of pre-treatment on biosolids pyrolysis. It was hypothesised that the removal or passivation of inherent metals in biosolids through acid pre-treatment could enhance the biochar quality, influence the formation path of chemical components in the bio-oil, and affect gas production during pyrolysis. Two pre-treatment scenarios were selected to include (i) biosolids acid treatment followed by water washing as a neutralisation step for selective demineralisation and (ii) biosolids acid treatment having residual acid unwashed for metal passivation. The specific objectives of this work were to study the effect of mild acid pre-treatment on (i) biosolids' physicochemical properties and thermal decomposition behaviour, (ii) pyrolysis product distributions, (iii) biochar quality with respect to carbon retention, calorific value, HMs concentration and bioavailability, and surface morphology, (iv) compositions of chemical compounds in the pyrolysis liquid to assess the chemical value of the bio-oil, and (v) compositions and evolution profile of non-condensable pyrolysis gases.

2. Materials and methods

2.1. Biosolids collection and sample preparation

Biosolids used in this study were collected from Mount Martha Water Recycling Plant, South East Water Corporation, Melbourne, Australia. The plant uses a dissolved air flotation process for sludge activation, then anaerobic followed by aerobic digestion for sludge treatment. The digested sludge is then dosed with polymer additives to coalesce the flocs, followed by mechanical dewatering in a centrifuge and drying in solar dryer shed. The biosolids employed in this study are the final solids from the dryer. The as-obtained biosolids were dried in an oven at 105 °C, ground, and sieved to 100–300 μm particle size before further use.

2.2. Biosolids pre-treatment

The pre-treatment procedure was as described in our previous work [17]. The biosolids were pre-treated using a 3% (v/v) sulfuric solution at a solid-to-liquid ratio of 1:10 (g/mL) at 25 °C under continuous stirring at 600 rpm for 1 h. These conditions were obtained from an earlier optimisation study [17]. At the end of the pre-treatment experiment, the slurry was vacuum filtered to separate into aqueous phase (filtrate) and solid residue (treated biosolids). The residue was divided into two portions. The first portion was washed many times with deionised water until the filtrate pH was near neutral to remove residual acid and other water-soluble inorganics. The second portion was used as obtained with no further water washing to study the effects of residual acid on biosolids pyrolysis performance. The raw (untreated) biosolids were denoted as RB, treated biosolids with water washing were denoted as TB, while treated biosolids with no water washing were denoted as TB_nw. The generation of large volumes of aqueous waste is a typical limitation of acid pre-treatment; however, our recent work has developed a closed-loop hydrometallurgical process for managing the generated aqueous acidic leachate stream via recycling and metal recovery [23]. The effect of pre-treatment on the pyrolysis behaviour of biosolids was assessed through Thermogravimetry analysis using a high-temperature TG/DSC Discovery series SDT650 equipment (TA instrument).

2.3. Pyrolysis experiments and products yield

Pyrolysis experiments were carried out in a quartz tubular fluidized bed reactor under atmospheric conditions. The details of the pyrolysis rig and reactor specifications can be found in our previous works [15, 29]. The pyrolysis procedure involves weighing 40 g of dry biosolids feed (RB or TB or TB_nw) into a clean, dry pre-weighed reactor. The reactor and its content were inserted vertically into a three-zone electrically controlled furnace with an average heating rate of 35 °C/min. The reactor and its content were continuously flushed with a stream of pure nitrogen to create an inert atmosphere before heating the reactor. The experimental setup is shown in Fig S1. Biosolids pyrolysis was conducted at three temperatures: 300, 500, and 700 ℃, which were selected to study the effect of pre-treatment on the product distribution and properties over a wide temperature range. During pyrolysis, a continuous stream of nitrogen flow required to achieve a gas velocity equivalent to 2.5 times the minimum fluidisation velocity was maintained using the Ergun correlation described in our previous work [30]. After reaching the desired temperature, the experiment was continued for 60 min, sufficient to complete the pyrolysis process. At the end of each experiment, biochar was collected from the reactor after cooling down to ambient temperature, and bio-oil was collected from the condensers. Non-condensable pyrolysis gas was continuously analysed online using micro-GC equipment connected to the pyrolysis gas cleaning units. Nine primary experiments were conducted, 3 samples by 3 temperatures. The pyrolysis product notations are distinguished by sample name-pyrolysis temperature, e.g., RB300 denoted Raw biosolids pyrolysed at 300 ℃. At least a single repeat experiment was conducted for all samples, and average data has been reported with error bars representing the standard deviation. Product yields were calculated using Eqs. (1)–(3).

$$\text{Biochar(wt\%)} = \frac{Weight\ \ of\ \ biochar}{Weight\ \ of\ \ biosolids\ \ feed}\ \ X100\% \tag{1}$$

$$\text{Bio} - \text{oil (wt\%)}\ = \frac{W_{CT\_after} - W_{CT\_before}}{Weight\ of\ biosolids\ feed}\ X100\% \tag{2}$$

$$\text{Gas(wt\%)} = 100\% - Biochar\ \ \ (wt\%) - Biooil(wt\%) \tag{3}$$

Where W_{CT} refers to the weight of the condensers and oil collecting tubes.

2.4. Products characterisation

2.4.1. Biochar

Proximate analysis of biosolids and their biochar were carried out using a TGA 8000 Perkin Elmer equipment, and the ultimate analysis was performed in a CHNS 2400 Series II Perkin Elmer equipment coupled to a thermal conductivity detector. Physicochemical properties such as pH and electrical conductivity (EC) were determined using a pre-calibrated platinum electrode probe. Higher heating value (HHV) was estimated using the correlation of Channiwala and Parikh [31] shown in Eq. (4). Bulk density of the biosolids and biochar samples was determined using the standard measuring cylinder method [30]. FTIR Spectra were captured in absorbance mode over a scanning wavelength of 4000–650 cm^{-1} at 32 scanning times and 4 cm^{-1} resolutions using Frontier FTIR Spectroscopy (Spectrum 100, Perkin Elmer). Scanning electron microscope (SEM) FEI Quanta 200, USA, was used to analyse the surface morphologies of biochar samples after coating with iridium using Leica EM ACE 600 sputter coating instrument. The SEM instrument was operated at 30 kV, and SEM images were captured at the same spot size (5.0) and magnification (×3000) to compare all samples' surface morphology. Brunauer–Emmett–Teller (BET) Surface Area Analysis was employed to estimate the surface area of the samples using Micromeritics TriStar II instrument.

The concentration of major elements in biosolids and biochar samples was measured using XRF analysis (S4 Pioneer Bruker AXS). Trace elements were measured using ICP-MS analysis following the acid digestion of the biosolids samples in aqua regia following the procedure described in Hakeem et al. [17]. Lastly, the potential soil bioavailable HMs concentration in biochar samples was measured using the diethylenetriamine pentaacetate (DTPA) acid extractable metal procedure [32]. Briefly, the extractant was prepared by weighing 1.97 g of DTPA, 1.47 g of $CaCl_2.2\ H_2O$, and 14.92 g of triethanolamine and dissolved in deionised water to make up 1 L solution. The pH of the solution was adjusted to 7.3 using concentrated HCl. Then 1 g of biochar sample was added to 10 mL of the pH-adjusted extractant solution, and the mixture was agitated at 250 rpm overnight at room conditions. The metal enrichment factor (MEF_i) and metal retention/recovery (R_i) in the biochar was estimated using Eqs. (5) and (6), respectively [17].

$$HHV\ \ \left(\frac{MJ}{kg}\right) = 0.3491C + 1.1783H + 0.1005S - 0.1034O - 0.0151N - 0.0211Ash \tag{4}$$

$$MEF_i = \frac{Metal_i\ \ concentration\ \ \left(\frac{mg}{kg}\right) in\ \ biochar}{Metal_i\ \ concentration\ \ \left(\frac{mg}{kg}\right) in\ \ biosolids} \tag{5}$$

$$R_i(\%) = MEF_i\ \ X\ \ biochar\ \ \ yield\ \ (wt\%) \tag{6}$$

2.4.2. Bio-oil compositions

Pure bio-oil oil samples collected from the condenser during pyrolysis were used for the analysis. Bio-oil samples were dissolved in DCM before analysis in a Gas Chromatography-Mass Spectrometry (GC/MS Agilent Technologies, GC/MSD 5977B, 8860 GC system) instrument. HP-5MS (19091S-433UI) capillary column (30 m length, 0.25 mm I.D. and 0.25 μm film thickness) was used in the GC/MS equipment, and the temperature program of the oven was as follows: isothermal hold at 45 °C for 3 min, ramp to 300 °C at 7 °C/min and isothermal hold at 300 °C for 5 min. Other conditions were 300 °C - injection temperature; 280 °C - MS transfer line; 230 °C - MS ion source; 1 μL - splitless injection volume; 23.0 mL/min - total inlet flow, and helium was used as the carrier gas. The relative composition of chemical compounds in each bio-oil sample was determined by peak area normalisation, denoted as peak area percentage [15]. For further analysis, the identified compounds in each bio-oil sample were categorised into different chemical groups such as oxygenated, nitrogenated, hydrocarbons, phenolics,

anhydrosugars, and sulfur-containing compounds. Acids, alcohols, aldehydes, esters, ethers, furans, and ketones were categorised into oxygenated, while pyrazine, pyridine, pyrrole, azole, amines, amides, and nitriles were categorised into nitrogenated. Phenols and their derivatives are phenolics, while saccharides and sugar alcohols are classified as anhydrosugars. Finally, olefin, paraffin, BTXS (benzene, toluene, xylene, and styrene), and PAHs were classified as hydrocarbons. This classification was used to provide insight into the chemical value of the bio-oil based on dominant platform chemical species and study the effect of pre-treatment on the distribution of the chemical compounds.

2.4.3. Pyrolysis gas compositions

The components and relative compositions (mol%) of the gas stream from each pyrolysis experiment were analysed online using a Micro-GC 490 (Agilent Technologies) instrument connected to the gas scrubbing unit from the pyrolysis reactor. The microGC has been calibrated with standard gases such as CO_2, CO, H_2, N_2, O_2 and C1-C4 hydrocarbon. Pyrolysis gasses were sampled every 4 min until the end of the experiment to identify and quantify the gas components. The gas evolution profile during the pyrolysis was obtained by plotting the relative gas compositions as a function of pyrolysis time.

3. Results and discussions

3.1. Effect of pre-treatment on biosolids physicochemical properties

The effect of H_2SO_4 pre-treatment on the physiochemical properties of biosolids is summarised in Table 1. The mild acid pre-treatment (3% H_2SO_4 at 25 ℃ for 60 min) of biosolids impacted the proximate compositions of the biosolids without substantial change in the ultimate compositions. Hence demineralisation mechanism dominated the pre-treatment process, which selectively removed inorganic matter. The percentage change in carbon contents was far lower than the percentage change in ash content of biosolids after pre-treatment. Specifically, there was a 40% and 20% decrease in ash content for TB and TB_nw, respectively and a 10% increase in the volatile matter for the treated samples. In contrast, the carbon, hydrogen, and nitrogen contents of the treated samples differ by less than 10% relative to the raw biosolids, attributed to the loss of acid-soluble light volatiles. The ash content decreased due to the substantial removal (>60%) of ash-forming elements (such as AAEMs, Fe, Al, and HMs) from the biosolids. Devolatilisation was slightly enhanced by pre-treatment due to the hydrolysis of recalcitrant organics, thereby increasing volatile matter from 57% in raw biosolids to over 63% in treated feeds.

There was also a considerable reduction in HMs concentration, particularly Cu and Zn, which are the major limiting HMs in biosolids for land application. Overall, there was about a 75% reduction in HMs concentration in the TB relative to RB. The intensity of demineralisation and HMs reduction, as well as other physicochemical changes, were lesser in TB_nw than in TB due to the subsequent water-washing step performed in the latter, which aided the removal of water-soluble inorganics and organic components. The HMs concentration (except Cu) in TB is within the concentration limit prescribed by Victoria EPA for C1-grade (least contaminant grade) biosolids for unrestricted land application [33]. The bioavailability of the residual HMs in TB is considerably low and can be an attractive material for direct land use in its current form [17]. However, other rapidly emerging contaminants in biosolids, such as per- and polyfluoroalky substances (PFAS) and microplastics, might still be present in TB. Our earlier work observed that sulfuric acid pre-treatment could not extract PFAS from biosolids; rather, the process concentrated PFAS in the treated solids due to volume reduction [23]. Therefore, the thermal treatment of TB via pyrolysis might be necessary to completely degrade all potential organic and microbial contaminants and produce quality biochar for land beneficiation and other high-value applications.

Table 1
Effect of pre-treatment on biosolids physicochemical properties.

Properties	Compositions/ Elements	Biosolids samples			
		RB	**TB**	**TB_nw**	**C1-grade biosolids***
Proximate analysis (wt% dry basis)	Moisture	1.9	1.8	0.8	
	Volatile matter	57.5	63.4	63.6	
	Fixed carbon	10.6	16.4	11.3	
	Ash	30.0	18.5	24.3	
Ultimate analysis (wt% dry basis)[a]	Carbon	35.4	36.4	32.9	
	Hydrogen	4.4	5.1	4.5	
	Nitrogen	5.6	5.6	5.5	
	Sulfur	0.9	2.3	7.4	
	Oxygen	23.8	32.1	25.5	
pH		6.8	6.0	2.0	
EC (μS/cm)		1885	2400	9385	
HHV (MJ/kg)[b]		14.4	15.1	14.2	
Bulk density (g/cm^3)		0.78	0.73	0.77	
Solids recovery (%)		-	80	95	
Carbon retention (%)[c]		-	82.3	88.3	
Major elements in ash (wt%)	Al	0.74	0.54	0.56	
	Ca	10.18	5.35	8.54	
	Cl	0.35	0.08	0.08	
	Fe	4.23	4.07	2.25	
	Na	0.12	BDL	BDL[d]	
	K	1.07	0.18	0.35	
	Mg	0.53	0.12	0.12	
	P	1.32	0.54	0.51	
	Si	2.69	3.29	2.91	
Demineralisation efficiency (%)[e]		-	38.6	19.0	
AAEMs removal efficiency (%)[f]		-	77.0	65.2	
Heavy metals (mg/kg)	As	2.5	1.3	1.9	20
	Cd	1.3	0.3	0.5	1
	Co	1.3	0.5	0.9	-
	Cu	690	220	500	100
	Cr	20	13	16	400
	Ni	18	7	12	60
	Mn	210	10	53	-
	Pb	20	18	17	300
	Zn	850	160	560	200
HMs removal efficiency (%)		-	76	35	

[a] Obtained by difference Oxygen = (100-C-H-N-S-Ash);
[b] Estimated using the correlation of Channiwala and Parikh (Eq. 4)
[c] $(Carbon\ content(wt\%) in\ treated\ feeds)/(Carbon\ content(wt\%)\ in\ raw\ biosolids) X\ Solids\ recovery(\%)$
[d] BDL – Below Detection Limit;
[e] Based on ash content reduction;
[f] Based on average Na, K, Mg, and Ca content reduction
* Biosolids grade for land application as prescribed by EPA Victoria [33].

Notably, there was an increase in sulfur content in TB_nw compared to the other two samples indicating the presence of high residual sulfur from H_2SO_4 pre-treatment without any post-treatment water washing. The sulfur from H_2SO_4 could react with organic matter in biosolids to form organosulfur compounds, which might initiate the release of sulfur-containing volatiles during pyrolysis. The FTIR spectra (Fig S2) of the treated biosolids confirmed the formation of organosulfur compounds such as C-S, C═S, S═O, and SO_2NH_2 groups. The water-washing neutralisation steps neutralised residual sulfuric acid and removed the precipitated metal sulfate salts, raising the treated solids' pH to 6.5 (Table 1). However, the water-washing process caused a loss of total solids with a solids recovery of 85% and carbon retention of 82% in TB compared to 95% solids recovery and 88% carbon retention in TB_nw. Pre-treatment had a negligible change on the calorific value of the feed materials due to the contrasting effect of ash and oxygen concentration on the HHV correlation (Eq. (4)); however, pre-treatment reduced the bulk density of the biosolids, which was more profound in TB due to the extra water washing step. The overall observation of the acid pre-

treatment process on the changes in the physicochemical properties of biosolids is comparable with the literature [8,18,19]. For instance, in the study of Liu et al. [18], 0.1 M H_2SO_4 pre-treatment of biosolids at ambient temperature for 12 h reduced the ash content by 12 wt% and increased volatile matter and carbon contents by ~10 wt% relative to the untreated biosolids. Tang et al. [19] using 5% HCl, 25 ℃ and 6 h for biosolids pre-treatment yielded 8 wt% decrease in ash content and ~5 wt% increase in volatile matter and carbon contents while nitrogen and hydrogen contents remained relatively unchanged compared to the raw biosolids. The current work used 3% H_2SO_4, 25 ℃ and 1 h to achieve 12 wt% reductions in ash content and 6 wt% increments in volatile matter while ultimate compositions were least impacted.

3.2. Effect of pre-treatment on biosolids thermal decomposition behaviour

The influence of pre-treatment on the pyrolysis behaviour of biosolids is illustrated by the various thermographs shown in Fig. 1. The DTG profile (Fig. 1(A)) occurs in three distinct degradation stages, which are: (I) dehydration (50–165 ℃), (II) devolatilisation of organic components (150–600 ℃), and (III) decomposition of recalcitrant carbonaceous materials and residual char organics (>600 ℃). In stage I, the dehydration peak attributed to the loss of moisture and light volatiles occurred at 100 ℃ with < 4% mass loss. The major mass loss (>50%) occurred in stage II over three degradation peaks at 250, 350, and 400 ℃, corresponding to the thermal decomposition of carbohydrates, lipids and proteins/biopolymers, respectively [34,35]. The last degradation stage III, with < 10% mass loss, peaked at 750 ℃ and was attributed to the degradation of recalcitrant organics, such as lignin, and a fraction of inorganics, usually carbonates. There were clear differences in the DTG thermograph of RB, TB, and TB_nw with respect to changes in maximum degradation temperatures and rate of weight loss. The maximum degradation temperature shifted to lower values in treated samples compared to the raw sample. In contrast, the raw sample's degradation rate was higher than the treated biosolids. For example, the maximum degradation temperature was 285 ℃ for RB, and it shifted to 245 ℃ for TB_nw and 260 ℃ for TB, and while the rate of weight loss was 5.5%/℃ for RB and it slightly decreased to 5.3%/℃ for TB and 4.3%/℃ for TB_nw. These differences can be attributed to the partial hydrolysis of organic matter and the removal of inorganics by the pre-treatment step, facilitating the thermal devolatilisation reactions at lower degradation temperatures. However, the pre-treatment process also resulted in the slight dissolution of organic matter, which decreased the overall quantity of volatile matter in the treated samples relative to RB, thereby reducing the rate of volatile degradation. The lower rate of TB_nw degradation compared to the other samples confirmed the formation of thermally stable metal sulfate salts, which inhibited organic

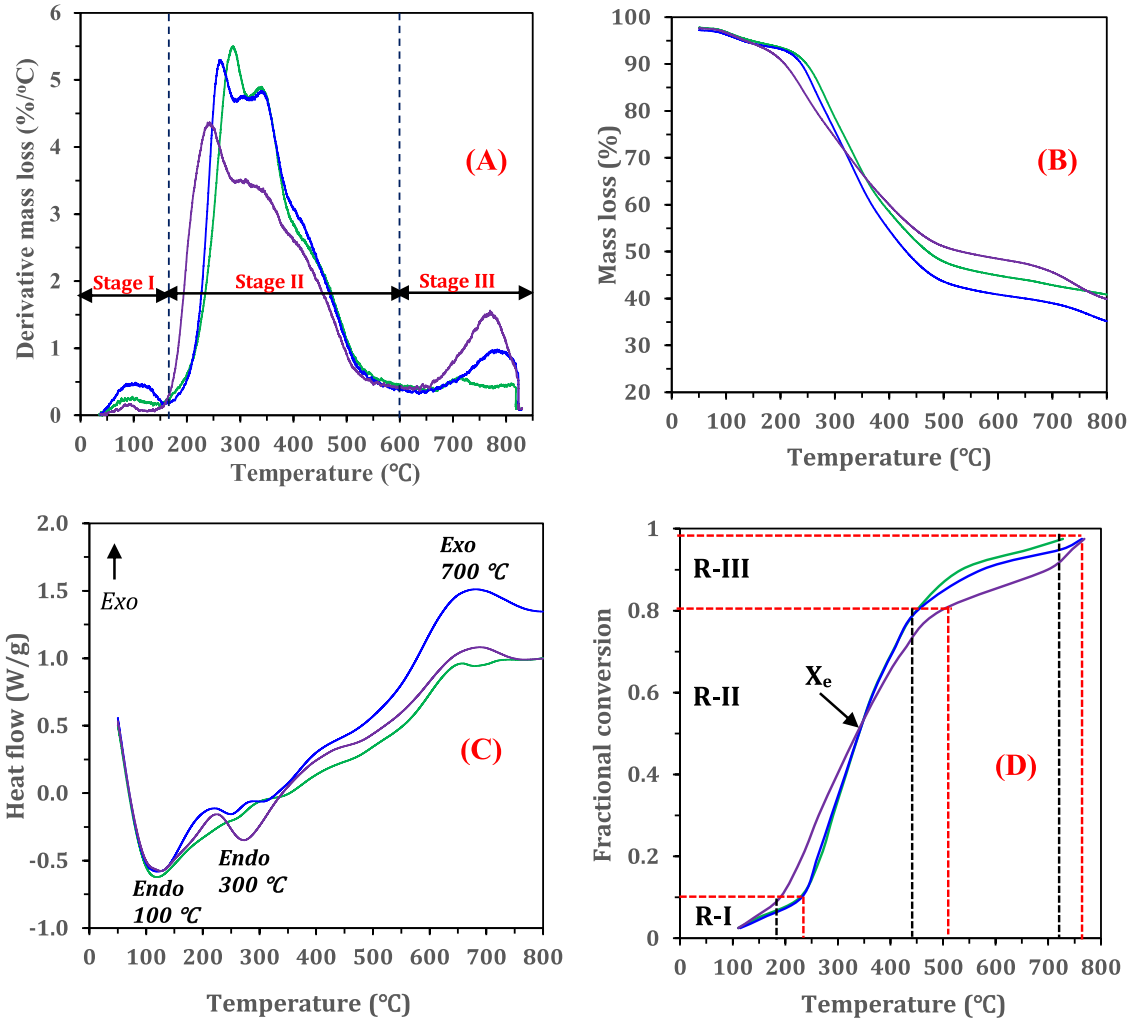

Fig. 1. Effect of pre-treatment on the thermal decomposition behaviour of biosolids (A) DTG thermograph showing decomposition peaks (B) TG mass degradation curve (C) DSC profile showing heat flow (D) plot of fractional conversion as a function of pyrolysis temperature.

matter conversion [36]. The TG curve (Fig. 1(B)) shows that the decomposition profile of TB and RB was closely similar with no overlapping, and at all temperatures, the degradation of TB was always higher than RB. This indicated that both samples have a similar organic matrix, and the lower ash content in TB was largely responsible for the higher mass loss at all temperatures. In contrast, TB_nw had a different degradation profile whose mass loss was faster than the other materials up to 320 ℃. Beyond this temperature, the mass loss was slower than in the other samples. The residual mass of RB and TB_nw was similar (40%), while that of TB was the lowest (35%).

Fig. 1(C) illustrates the DSC curve of the biosolids samples showing the thermal energy flow as a function of pyrolysis temperature. Pyrolysis is an endothermic process where external energy is needed to break chemical bonds and decompose major biochemical components into primary decomposition products. From Fig. 1(C), two distinct endothermic peaks occurred at 100 ℃ and 300 ℃, corresponding to loss of moisture and organic devolatilisaiton, respectively. After the initial transformation up to 350 ℃, the energy needed to heat the feed materials began to decline, and the decrease of heat flow with increasing pyrolysis temperature from 350 to 600 ℃ was almost linear. During this stage, there are traces of broad endotherms indicating that the decomposition of organic matter at 300–600 ℃ required minimal thermal energy. However, the non-distinct endotherms made attributing the degradation behaviour to specific organic components difficult. Beyond 600 ℃, a small exothermic spike was observed occurring at 650–750 ℃ attributed to the decomposition of carbon refractories such as aromatic ring, N-alkyl long chain structures, and carbonates with the release of CO_2 [37,38]. The intensity of the endothermic peak at 300 ℃ in TB_nw suggests that the thermal energy required to decompose its organic structure is higher. The infusion of sulfuric acid might have changed the organic structure of TB_nw to a thermally recalcitrant matrix through the formation of stable metal sulfate salts, consistent with observations reported in other works [18,39].

The iso-conversional temperature required for the pyrolysis of the three biosolids samples at the same heating rate (20 ℃/min) is shown in Fig. 1(D). The figure indicates that the pyrolysis conversion of biosolids occurred over at least three kinetic regimes: i) $\leq$ 10% conversion occurring at 100–240 ℃ (R-I), ii) 10–80% conversion occurring at 240–500 ℃ (R-II), and iii) $\geq$ 80% conversion at 500–800 ℃ (R-III). These three kinetic regimes denoted dehydration, primary devolatilisation, and secondary devolatilisation and char cracking stages. However, the temperature required for each conversion stage differs for individual samples. For example, 10% conversion of TB_nw occurred at 190 ℃ and about 230 ℃ for both RB and TB, suggesting that the dehydration stage occurred faster in TB_nw compared to the other two samples. The faster conversion kinetics of TB_nw continued into the primary devolatilisation stage up to 50% conversion, after which the rate was slower than RB and TB. Meanwhile, both RB and TB showed similar kinetics, up to 80% conversion, suggesting that the organic structure of both samples is identical. The slightly higher conversion rate of RB beyond 80% can be attributed to the role of native inorganic minerals, which promoted the cracking of recalcitrant organic matter. Notably, the pyrolysis temperature required to achieve 50% conversion was largely similar for all samples (340 ℃), as the conversion rate of all samples overlapped at that temperature (indicated by X_e in Fig. 1(D)). Overall, the required pyrolysis temperature was lowest for TB_nw at any given conversion $<$ 50% and was highest at any given conversion $>$ 50%.

3.3. Pyrolysis products distribution: effect of pre-treatment and temperature

The product distribution of raw and treated biosolids at 300–700 ℃ is shown in Fig. 2. The product yields are expressed in dry feed weight to compare the influence of the temperature and pre-treatment on pyrolysis product distributions (Fig. 2(A)). According to Fig. 2, with increasing pyrolysis temperature (from 300 to 700 ℃), biochar yields decreased while bio-oil and gas products yield increased irrespective of feed material. This trend in product distribution as a function of pyrolysis temperature is consistent with extant literature [29,30,40]. With increasing pyrolysis temperature, mass and heat transfer rates are faster, and several thermolysis decomposition reactions are enhanced with the rapid cleavage of chemical bonds. For all samples, the effect of pyrolysis temperature on biosolids devolatilisation was profound between 300 and 500 ℃ compared to that between 500 and 700 ℃. Nevertheless, bio-oil and gas products yield monotonically increased with temperatures up to 700 ℃, indicating that biosolids contain recalcitrant organic fraction requiring higher temperatures to devolatilise. For example, during RB pyrolysis, the conversion was 28.8% at 300 ℃; it increased to 49.7% at 500 ℃ and 58.6% at 700 ℃. A similar trend can be observed for TB and TB_nw. The DTG profile in Fig. 1(A) showed that most of the organic components in biosolids volatilised at temperatures between 200 and 500 ℃. There were only slight improvements in bio-oil and gas yield by raising the temperature to 700 ℃.

Pre-treatment had a clear effect on pyrolysis product distribution. From Fig. 2(A), pyrolysis of TB produced lower biochar yield (38.2–65.6 wt%) than that from RB (41.4–71.2 wt%), and the biochar yield from TB_nw (43.0–68.7 wt%) was found to be between the yields from RB and TB. In contrast, bio-oil yield from TB (24.7–42.6 wt%) was higher than that from RB (20.6–37.0 wt%) and TB_nw (19.6–36.8 wt%). Removal of ash-forming elements from biosolids and partial hydrolysis of the organic matter by H_2SO_4 pre-treatment improved the devolatilisation of TB to produce more bio-oil and less char residues compared to other biosolids samples. It has been indicated that trace levels ($<$1 wt%) of certain ash components in biomass have significant catalytic effect during pyrolysis, which can decrease bio-oil yield considerably [41]. From Fig. 1(A), TB_nw had the least conversion of all biosolids samples producing the highest biochar yield at 500 and 700 ℃. The residual sulfuric acid in TB_nw can catalyse crosslinking and polycondensation reactions at higher temperatures to form extra char, thereby increasing biochar yield [42]. The effect of pre-treatment was prominent on the distribution of biochar and bio-oil fractions, suggesting that the removal of inorganics had a remarkable influence on the thermal devolatilisation of organic matter in biosolids. Depending on the metal species and chemical form, mineral components have been shown to play various catalytic roles in releasing pyrolytic volatiles from organic matter [26,43]. The extent of the interaction of mineral matter on organic matter conversion during biosolids pyrolysis has been elucidated in another work [8]. The gas product yield increased with increasing pyrolysis temperature and was higher for RB and TB_nw than for TB. The catalytic effect of the inherent inorganics in RB and residual acid in TB_nw facilitated gas production through secondary cracking and dehydration reactions, respectively.

Fig. 2(B) shows the pyrolysis product yield expressed on volatile solids (VS) or dry-ash-free basis to discount the effect of ash matter on product distribution as well as understand the real impact of pre-treatment on the downstream pyrolysis conversion of VS. At all pyrolysis temperatures, RB and TB had a similar yield of bio-oil in the range of 30–53 wt%, and biochar yield (30–59 wt%) was only similar for both samples at 300–500 ℃. However, gas and biochar yield varies substantially for RB and TB at 700 ℃. This indicates that VS conversion to bio-oil was not negatively impacted by demineralisation as in the case of TB. In contrast, biosolids pre-treatment without the water neutralisation step, as in TB_nw, negatively impacted VS conversion to bio-oil during pyrolysis at all temperatures. The higher biochar yield at 500 and 700 ℃ for treated biosolids compared to the RB clearly indicates the char cracking role of native mineral matter during biosolids pyrolysis. The presence of mineral matter in RB caused a substantial cracking of recalcitrant volatiles at 700 ℃ to decrease biochar yield and increase gas yield. Consequently, RB conversion was 84% against 75% for treated biosolids. The elevated VS conversion attributed to the internal minerals in RB caused a decrease in fixed carbon and organic matter retention of

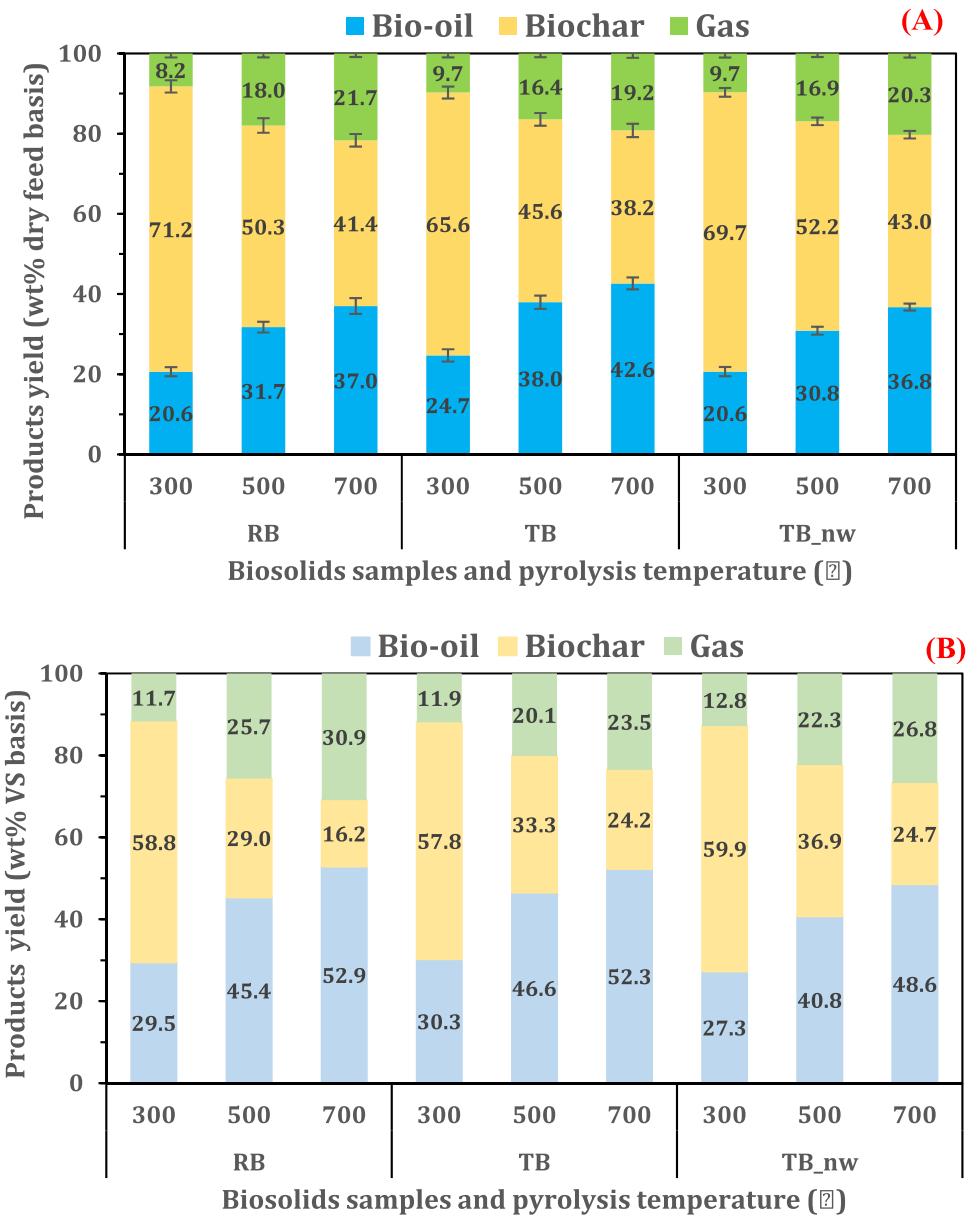

Fig. 2. Effect of pre-treatment and temperature on biosolids pyrolysis product distribution (A) expressed on a dry feed weight basis (B) expressed on volatile solids (dry-ash-free) basis.

the resulting biochar. In contrast, the lower conversion of VS in treated biosolids increased fixed carbon content and organic matter retention in the biochar. The higher biochar yield from the treated samples suggests that the pre-treatment process caused a reduction of thermally labile VS through the dissolution of acid-soluble organics and the loss of total solids during the process. This observation was confirmed by the 80–95% solids recovery and 82–88% carbon retention in treated biosolids relative to RB (Table 1). Besides the loss of total solids and light volatiles during pre-treatment, the residual organic structure might also be impacted by pre-treatment, increasing the stable VS fraction as indicated by the higher fixed carbon contents in treated biosolids. In sum, pre-treatment weakened the pyrolysis conversion of biosolids VS to gas product only at 700 ℃.

Under the conditions of this work, there could be more than one mechanism through which acid pre-treatment influenced biosolids organic matter devolatilisation to produce higher bio-oil and lower biochar compared to RB. Perspectives on how biosolids' devolatilisation could be enhanced by acid pre-treatment with water washing step (as in TB) have been provided.

i) The substantial reduction of ash content by pre-treatment increased volatile matter concentration in TB. Since the volatile matter content per solid mass is higher in TB than RB, the pyrolysis of equal amounts of TB and RB implies more volatiles per unit TB mass is available for thermal conversion to bio-oil. The lower biochar yield in TB is due to reduced ash content since ash components are largely retained in the biochar. The proximate compositions of the biosolids changed substantially after pre-treatment, with a major opposite shift in the volatile matter and ash matter contents (Table 1).

ii) During pre-treatment, complex organic components in biosolids can be hydrolysed into simpler components through the disruption of O-H bonds by H^+ from acid solution and surface deprotonation reaction causing the cleavage of carbonyl groups in protein and carbohydrate structures [20,22]. The partially hydrolysed organic macromolecules in TB are thermally less stable, and their characteristics decomposition temperature occurs in a lower region than untreated biosolids

Table 2
Effect of pre-treatment on biochar physicochemical properties.

Pyrolysis temperature (°C)	300			500			700		
Biosolids samples	RB	TB	TB_nw	RB	TB	TB_nw	RB	TB	TB_nw
Proximate analysis (wt% dry basis)									
Moisture	0.37	0.47	0.45	0.80	0.65	0.84	0.84	0.91	0.89
Volatile matter	46.16	52.11	50.69	29.28	30.67	35.67	20.07	21.70	16.71
Fixed carbon	14.66	18.45	13.28	17.62	27.66	17.15	19.99	31.32	27.26
Ash	38.82	28.97	35.57	52.31	41.02	46.35	59.10	46.06	55.15
Ultimate analysis (wt% dry basis)									
Carbon	39.35	45.08	40.07	32.82	41.67	35.34	30.41	37.27	30.21
Hydrogen	3.18	3.57	2.80	1.01	1.50	1.08	0.29	0.83	0.48
Nitrogen	6.55	7.35	6.39	5.47	5.63	5.21	3.25	4.83	4.01
Sulfur	0.89	2.58	6.13	0.58	3.12	6.06	0.65	3.14	7.32
Oxygen[a]	11.22	12.45	9.04	7.81	7.07	5.97	6.30	7.87	2.84
Other properties									
O/C	0.21	0.21	0.17	0.18	0.13	0.13	0.16	0.16	0.07
H/C	0.97	0.95	0.84	0.37	0.43	0.37	0.11	0.27	0.19
pH	5.8	5.5	4.1	7.8	6.8	6.3	9.8	9.4	9.6
EC (μS/cm)	722	1042	2614	305	1500	1868	2160	3218	2902
Bulk density (g/cm^3)	0.79	0.74	0.69	0.80	0.78	0.67	0.83	0.70	0.65
HHV (MJ/kg)[b]	15.49	18.19	16.13	10.71	14.95	12.54	9.07	12.44	10.33
Fuel ratio (FC/VM)[c]	0.32	0.35	0.26	0.60	0.90	0.48	1.00	1.44	1.63
Organic matter retention (%VS)[d]	58.8	57.8	58.6	29.0	33.3	36.8	16.3	24.2	24.7

[a] Obtained by difference, i.e. O = 100-(C+H+N + S+Ash);
[b] Estimated by the correlation of Channiwala and Parikh [31] (Eq. 4);
[c] Fuel ratio was estimated by dividing the fixed carbon content (wt%) by the volatile matter content (wt%) in each sample;
[d] Calculated by dividing the volatile solids (VS) in biochar (Biochar yield (wt%)–ash content (wt%)) by the corresponding VS in the respective feedstock (100 (wt%)–ash content (wt%)).

(The TGA/DTG curve confirmed the shift to lower degradation temperature) (Fig. 1(A)).

The results of this work provide insight into the impact of acid pre-treatment on biosolids pyrolysis product distribution under a wide range of temperatures. However, the findings cannot sufficiently identify the specific organic chemical bonds and components being transformed during pyrolysis, aided or inhibited by pre-treatment. Further studies are needed to comprehensively understand the pre-treatment process and the exact mechanisms through which organic matter devolatilisation occurs to increase bio-oil yield.

3.4. Effect of pre-treatment on biochar quality

3.4.1. Physicochemical properties

The physicochemical properties such as proximate and ultimate analyses, caloric value, pH, carbon retention and bulk densities of the resultant biochar obtained from the three biosolids feed samples at 300–700 °C are summarised in Table 2. Generally, volatile matter (VM) decreased, while fixed carbon (FC) and ash content increased in all biochar samples with increasing pyrolysis temperature. However, the increase in FC was negatively influenced by higher ash contents in biochar as the metal oxides in the ash can further oxidise FC, particularly at higher temperatures. During pyrolysis, thermally labile organic matter in the biosolids is removed, leading to substantial volume reduction. As a result, recalcitrant organic matter and inorganic matter are concentrated in the biochar. Increasing pyrolysis temperature increased the intensity of organic matter degradation and inorganic matter retention. The reduction of VM with increasing temperature had a consequential decrease in the ultimate compositions (C, H, N, O) of the biochar through dehydration, deoxygenation, decarboxylation, and denitrogenation reactions. Pre-treatment had clear effects on the proximate and ultimate compositions of the biochar samples. At all pyrolysis temperatures, biochar obtained from treated feeds had lower ash contents and higher FC than RB-biochar due to the prior removal of the ash-forming elements via the pre-treatment demineralisation process. TB-derived biochar had the highest VM and FC increase, and the lowest ash contents decrease compared to corresponding biochar obtained from other biosolids feeds, albeit at the cost of biochar yield. Pre-treatment with water neutralisation steps retained higher organic matter in the biochar (24–58%), supported by the higher carbon contents and calorific value in the TB-derived biochar relative to RB and TB_nw biochar (Table 2). Also, the fuel ratio of TB biochar was higher than RB-biochar, particularly at 700 °C; the fuel ratio of treated biosolids biochar was higher by 44–63% than RB-biochar. It is then suggested that removing minerals before pyrolysis can be a promising approach for strengthening biochar carbon-sequestration and energy-recovery potential. Also, the lower ash contents in the TB-derived biochar can enhance the biochar-carbon resistance to thermal and chemical oxidation, thereby increasing the carbon stability, as demonstrated in previous work [8]. However, the increase in sulfur contents in the biochar may be an undesired outcome of the pre-treatment process, particularly when the sulfuric acid pre-treatment is not followed by the water-washing neutralisation step, as in TB_nw. Nevertheless, sulfur is an essential plant micronutrient in biochar for land application, and the pre-treatment can enrich the derived biochar of sulfur contents compared to RB-biochar.

The elemental H/C and O/C ratio is typically used to measure biochar aromaticity and biochemical stability and can be correlated to pyrolysis temperature [44]. The decrease in the H/C ratio indicated higher biochar aromaticity due to the strong degree of carbonisation with increasing pyrolysis temperature [40]. Biochar produced at higher temperatures and from pre-treated biosolids had aromatic and hydrophobic structures through the loss of oxygen-containing functional groups (such as hydroxyl and carboxyl). Nan et al. [8] also observed that removing inherent minerals from sewage sludge via acid pre-treatment facilitated the disappearance of oxygen-containing functional groups such as C═O, O═C–O, and C–O, while promoting C–C/C═C bonds, indicating higher aromatisation of biochar. Pyrolysis temperature plays an important role in shaping biochar's surface chemistry and organic structure. At lower temperatures (<500 °C), the hydrogen-bonding network in the organic compounds is eliminated, and hydroxyl groups are oxidised to carboxyls. At higher temperatures, methylene groups are heavily dehydrogenated to aromatic structures [45]. The bulk (or apparent) densities of the biochar obtained at 300–700 °C from the three biosolids feed samples were found to vary substantially. Generally, there was a monotonic increase in bulk density with increasing pyrolysis

Table 3
Effect of pre-treatment and pyrolysis temperature on metal concentration in biochar.

Temp. (℃)	300			500			700		
Feed samples	RB	TB	TB_nw	RB	TB	TB_nw	RB	TB	TB_nw
Major metal oxides (wt%)									
Al_2O_3	2.1	1.7	1.7	3.0	2.5	2.0	3.4	2.8	2.7
CaO	14.3	8.7	12.9	17.3	10.8	14.2	18.8	11.7	15.9
Fe_2O_3	6.6	4.6	4.0	8.0	6.0	4.7	8.2	6.4	5.0
K_2O	1.5	0.3	0.5	1.8	0.4	0.6	1.9	0.4	0.6
MgO	1.1	0.3	0.3	1.6	0.5	0.4	1.8	0.5	0.5
Na_2O	0.5	BDL[a]	BDL	0.7	BDL	BDL	0.7	BDL	BDL
P_2O_5	3.4	1.5	1.3	4.4	1.9	1.4	4.8	2.1	1.7
SiO_2	7.7	10.6	8.6	10.6	14.9	8.9	11.9	16.0	11.4
Heavy metals (mg/kg)									
As	3.0	2.0	2.5	3.5	2.4	3.0	2.1	1.7	1.9
Cd	1.8	0.5	0.7	2.5	0.7	1	1.8	0.8	0.8
Cr	30	15	23	47	28	32	35	30	22
Cu	890	1100	1600	950	1200	1800	1200	1400	1900
Ni	26	10	17	38	13	24	29	16	16
Pb	29	25	21	37	40	34	40	40	36
Zn	1300	400	770	1500	580	970	1600	530	930

[a] BDL – Below detection limit

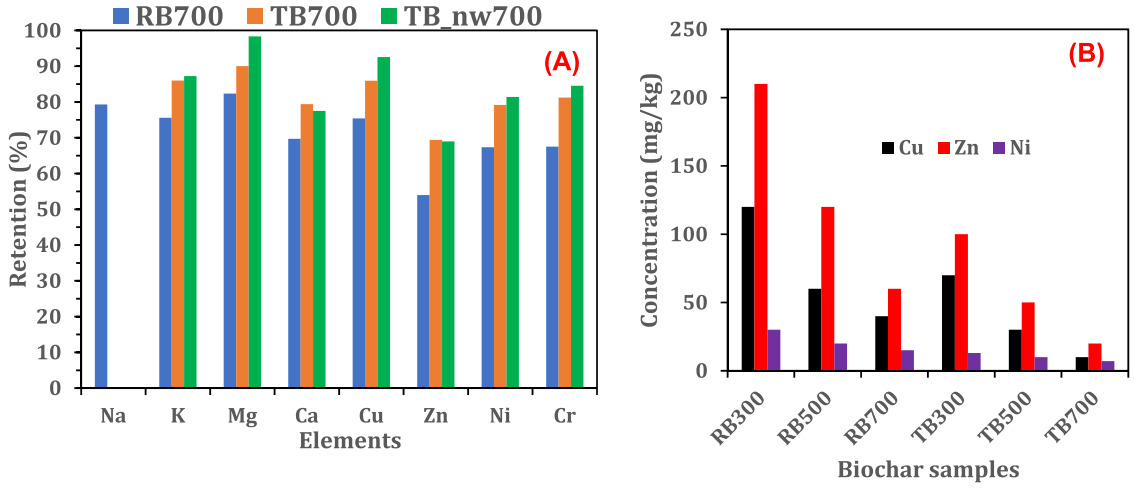

Fig. 3. Effect of pre-treatment on (A) metal retention in biosolids biochar at 700 ℃ (B) bioavailable HMs concentration in biosolids biochar.

temperature reflected by the extent of volume reduction caused by pyrolysis. The bulk density of the RB-biochar was the highest, followed by TB_nw and TB-biochar, which is reflective of the lower ash content in treated biosolids relative to raw biosolids at a given pyrolysis temperature. Lastly, the pH of the biochar was observed to generally increase with increasing temperature largely due to the destruction of acidic functional groups and the increase in the concentration of basic functional groups such as char-N as well as metal oxides in the ash contents. Biochar produced from TB_nw at 300 ℃ was more acidic (pH 4) than biochar from other biosolids samples (pH 5.5–5.8) due to residual sulfuric acid in TB_nw. However, the pH of all biochar samples was similar at 700 ℃ suggesting the inherent acid in TB_nw has no influence on the resultant biochar pH, possibly because acidic metal sulfate salts have been cracked into normal metal sulfate or oxides form.

3.4.2. *Metals concentration, retention, and bioavailability*

The effect of pre-treatment on the concentration of inorganic elements in biochar was assessed. The compositions and concentration of metal oxides and HMs in the raw and treated biosolids-derived biochar produced at 300–700 ℃ are summarised in Table 3. The major ash-forming elements enriched in the biochar are oxides of Ca, Si, Fe, P, Al, K, Mg, and Na in decreasing order. Expectedly, the metal concentration increased with increasing pyrolysis temperature (decreasing biochar yield). The metal concentrations were highest for the RB biochar samples containing the full spectrum of metal components. The prior removal of inorganic elements during pre-treatment substantially reduced the final concentration in the treated biosolids biochar. Notably, Na removal in biosolids via pre-treatment was almost 100%; consequently, Na_2O was only detected in RB biochar and was below the detection limit in all treated biosolids biochar samples. According to Fig. 3(A), the metal contents in the respective biosolids feed were largely retained in their derived biochar with a retention rate of $> 90\%$, confirming the thermal stability of the metal species at the pyrolysis conditions. However, at the highest pyrolysis temperature (700 ℃), there appears to be some volatilisation of AAEMs, particularly Ca and K, attributed to the decomposition of Ca-containing minerals such as $CaCO_3$ in the case of RB and $CaSO_4$ hydrates in the case of treated biosolids. In addition, the sublimation of KCl at high temperatures may cause K loss from the biochar [29]. Moreover, recalcitrant organics bonded to mineral matter may decompose at high temperatures leading to the release of metal species to the gas phase, lowering their recovery in the biochar [46].

Heavy metals are limiting contaminants in biosolids and their derived char, particularly for land application purposes. The HMs concentration in the biochar obtained from the three biosolids samples at 300–700 ℃ is shown in Table 3. The concentration generally increases with temperature with an enrichment factor of at least 1.2 times the concentration in the parent biosolids at 300 ℃ and up to 2.5 times at

700 ℃. Up to 500 ℃, there was an upward trend in the increase in the HMs concentration. However, at 700 ℃, there was a decline in the concentration of the metals attributed to the rise in the thermal volatilities of certain elements. Specifically, at 700 ℃, less than 50% of As and Cd were retained in the biochar, and Zn retention was less than 70%. Zhang et al. [47] reported similar observations during sewage sludge pyrolysis, with Hg being completely partitioned in the oil and gas product fractions as low as 300 °C while Cd and As had less than 10% recovery in the biochar at 650 °C. At 700 °C, the thermal volatilities of HMs can be ranked as Cu < Cr < Ni < Pb < Zn < As = Cd, suggesting that Cu, Cr, and Ni were least involved in migration during biosolids pyrolysis. This observation was similar to that reported in previous works [29,47]. Cu had the highest retention in biochar due to the high affinity of Cu to organic matter [17]. The higher organic matter retention in TB/TB_nw biochar also explains the higher Cu concentration in treated biosolids biochar compared to RB biochar. The poor removal of Pb with sulfuric acid resulted in the inconsequential effect of pre-treatment on Pb concentration in the biochar obtained from all samples. The concentration of all other HMs was lower in treated biosolids biochar compared to RB biochar, with the lowest for TB biochar. However, the enrichment factor for a given HM was higher in TB biochar than in RB biochar. The low ash content in TB weakens the dilution effect resulting in higher MEF. For instance, in biochar obtained at 500 ℃, Cd concentration increases by 1.9 times for RB and 2.3 times for TB; similarly, Zn enrichment was 1.8 for TB and 3.6 for TB. Besides the reduction of metal concentration by pre-treatment, there was an increase in the stability of the metal as their recovery in the biochar was higher for treated samples than the RB (Fig. 3(A)). The removal of acid-exchangeable (ionisable) and reducible metal (bound to carbonates and Fe-Mn oxides) fractions during pre-treatment facilitated the transformation and stabilisation of the remaining HMs in the treated samples to oxidisable (bound to organic matter) and residual fractions (bound to silicates) [48]. Therefore, stabilising HMs in the TB and TB_nw biochar compared to RB biochar can reduce the undesired migration of HMs into oil and gas product fraction during biosolids pyrolysis.

The reduction of HMs concentration and the increased metal stability in the biochar facilitated by pre-treatment may not be enough indication of the potential toxicity of the residual HMs. Therefore, DTPA-plant

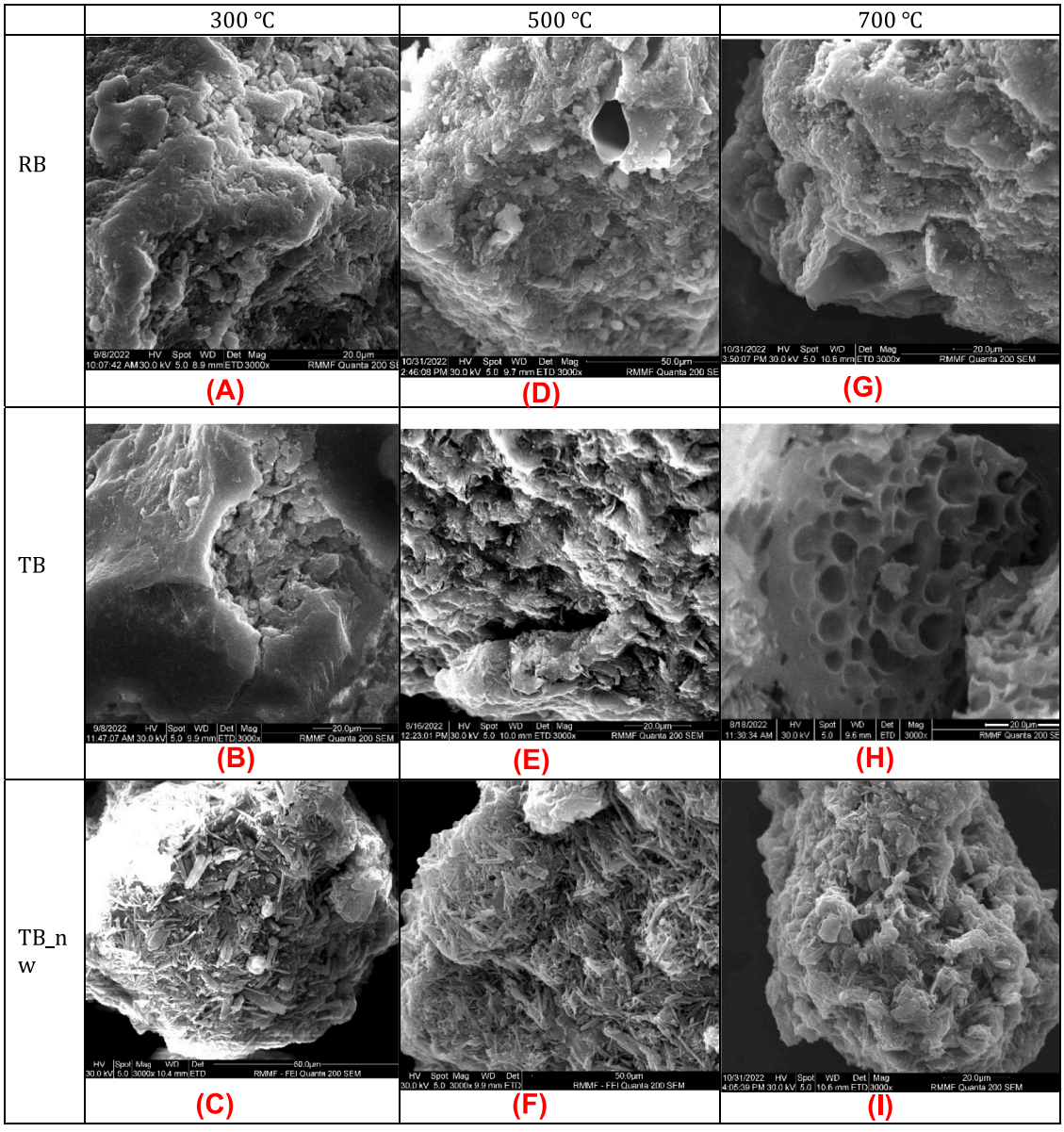

Fig. 4. Effect of pre-treatment and temperature on the surface morphology of biosolids biochar (A) RB300 (B) TB300 (C)TB_nw300 (D) RB500 (E) TB500 (F) TB_nw500 (G) RB700 (H) TB700 (I) TB_nw700.

available HMs concentration was assessed, and the result showed that pre-treatment drastically reduces the bioavailable metal concentration in the biochar (Fig. 3(B)). Specifically, at 500 ℃, the DTPA-extractable Cu concentration from RB biochar was 60 mg/kg, while it was 20 mg/kg for TB biochar. Similarly, Zn bioavailable concentration in TB biochar was reduced by at least 50% compared to RB biochar at the same pyrolysis temperature. The effect of pre-treatment follows a similar trend for Ni bioavailable concentration reaching about 7 mg/kg in TB700 compared to 15 mg/kg in RB700. The higher organic matter retention and surface functional groups in TB biochar could promote organometallic complexation reaction, thereby enhancing HMs immobilisation in the char matrix and decreasing the extractable metal concentrations [49].

3.4.3. Morphological properties

The SEM imaging of the biochar obtained from raw and treated biosolids samples at 300–700 ℃ is shown in Fig. 4. There was a clear distinction in the image of the samples, highlighting the effect of pre-treatment and pyrolysis temperatures on biochar surface morphology. The image of the biochar obtained at 300 ℃ (Fig. 4(A-C)) showed a bulky structure with particle shrinkage resulting from the dehydration and decarboxylation of organic matter. The char sample from RB and TB appeared similar (Fig. 4(A&B)), and the biochar sample from TB_nw (Fig. 4(C)) had a flaky structure with a surface covering arising from the acidic metal sulfate salts. At 500 ℃, the image of the char samples (Fig. 4(D-F)) showed a matured organic conversion with the compact structure becoming disintegrated into small fragments; however, the pore structure is not well developed with traces of pore openings. The char from TB_nw still showed the thermally stable metal sulfate salts coverings, limiting the full development of the pores (Fig. 4(F)). At 700 ℃ (Fig. 4(G-I)), organic compounds have been completely degraded, and the char cracking reaction removed residual volatiles, opening up pores within the char matrix and exposing the char surface. TB biochar has a strong pore development (Fig. 4(H)) due to enhanced devolatilisation and lower ash residues. The RB700 (Fig. 4(G)), due to its high ash content, had poor pore structure development attributed to the creation of stable organometallic compounds within the aromatic structures, which are recalcitrant to thermal volatilisation at 700 ℃ [29]. It has been suggested that high levels of ash-forming minerals in biosolids would require higher pyrolysis temperatures for their biochar pore structure to be fully developed compared to low-ash-containing biomass biochar [6]. Hence, reducing the ash minerals in biosolids by mild sulfuric acid pre-treatment was beneficial in producing biochar with a porous structure, albeit the effect was profound only at 700 ℃. However, the presence of residual acid and acidic metal sulfate salts inhibited volatile removal and caused pore blockage, as observed in the SEM images of TB_nw.

The BET-specific surface areas and average pore volume of the biochar samples are summarised in Table 4. At 300 ℃, the surface area (15–25 m^2/g) of the biochar from all feed samples was largely similar; however, the pore volume of TB (0.024 cm^3/g) was almost double of the RB (0.012 cm^3/g) supporting the elevated rate of inorganic removal by pre-treatment and organic matter removal from the bulk of TB sample during pyrolysis. Increasing the pyrolysis temperature to 500 ℃ increased the biochar surface area by at least 40%, reaching 27 m^2/g for RB and 40 m^2/g for TB, and a further increase in temperature to 700 ℃ increased the surface area to 55 m^2/g for RB and 107 m^2/g to TB. The 2-fold higher surface area of TB-biochar compared to RB-biochar was supported by the improved pore structure development of TB biochar, as shown in Fig. 4(H). Higher surface area and pore volume are indicative of the stability of the char structure, which can enhance their application in catalysis and adsorption [6]. The pore size distribution indicates that the biochar materials are largely mesoporous with pore width in the 2–50 nm range. However, the relatively lowest pore width in the case of TB_nw indicates possible pore blockage by the poorly soluble metal sulfate salt, particularly $CaSO_4$ hydrates that covers the surface as observed under the SEM imaging.

3.5. Effect of pre-treatment on bio-oil compositions

The chemical compositions identified through the GC/MS analysis of the bio-oil obtained from the pyrolysis of raw and treated biosolids are summarised in Table 5. The results showed that the bio-oil is a complex mixture of various chemical compounds grouped into oxygenates, nitrogenated compounds, sulfur-containing, and hydrocarbons. Temperature and pre-treatment considerably affect the evolution of volatile organic compounds in the bio-oil. Generally, for all biosolids samples, the yield of nitrogenated and oxygenated compounds decreased with increasing pyrolysis temperature, while hydrocarbons and phenol yield increased with temperature. The effects of pre-treatment on the distribution of chemical components in the bio-oil varied with pyrolysis temperature. For instance, pre-treatment enhanced hydrocarbon production from 20% in RB to 30–35% in treated biosolids at $\geq$ 500 ℃, whereas anhydrosugars yield was increased from 2.1% in RB to 4.5% in TB only at 300 ℃, while phenolics yield was similar for all bio-oils at all temperatures.

The bio-oil obtained at 300 ℃ consists mainly of high molecular weight nitrogenated and oxygenated compounds, with major chemical species being *N*-heterocyclics and ketones. Nitrogenated compounds in bio-oil originated from the thermal devolatilisation of proteins, while ketonic compounds are from the primary decomposition of carbohydrates. *N*-heterocyclics could be formed by dehydrogenation of the amino group present in proteins and nucleic acids in biosolids and through the addition of HCN and/or NH_3 to benzene/toluene aromatic ring during pyrolysis [50]. Dehydration and decarboxylation of organic matter are prominent thermolysis reactions at lower temperatures resulting in the formation of high-molecular-weight reactive oxygenate fragments such as R–CHO, R–C–O–R, R–CO–OH, and R–O–R [51]. Pyrolysis at 300 ℃ was selective for producing a few kinds of *N*-heterocyclics, amides/amines, and ketones, irrespective of the biosolids feed

Table 4
Surface properties of biochar samples.

Pyrolysis temperature (℃)	Feed samples	Surface properties		
		BET specific surface area (m^2/g)	BJH average pore volume (cm^3/g)	BJH average pore width (nm)
300	RB	15.2	0.012	7.94
	TB	25.2	0.024	8.00
	TB_nw	20.5	0.015	7.84
500	RB	26.9	0.021	8.67
	TB	43.7	0.030	8.81
	TB_nw	32.9	0.017	8.22
700	RB	55.3	0.039	7.65
	TB	106.9	0.061	8.54
	TB_nw	72.5	0.043	7.03

Table 5
GC/MS analysis showing the chemical composition of the bio-oil samples.

Bio-oil compositions									
Pyrolysis temperature (℃)	**300**			**500**			**700**		
Biosolids samples	**RB**	**TB**	**TB_nw**	**RB**	**TB**	**TB_nw**	**RB**	**TB**	**TB_nw**
Compounds	Peak Area (%)								
Pyrazine	14.1	2.9	16.3	-	-	2.3	4.5	-	-
Pyridine	8.3	6.4	8.5	3.0	1.5	2.3	1.7	1.0	8.5
Pyrrole	3.4	0.4	-	8.2	1.4	0.4	1.6	5.7	0.5
Azole	0.3	0.2	-	0.9	6.3	0.9	9.0	8.0	0.5
Amines	5.3	5.8	16.9	3.4	2.0	0.6	1.3	0.4	4.6
Amides	19.3	17.6	8.5	7.4	4.8	2.1	4.2	2.3	1.6
Nitriles	1.8	1.1	3.2	4.5	7.1	7.2	3.8	5.9	6.5
Total Nitrogenated	**52.5**	**34.4**	**53.4**	**27.3**	**23.0**	**15.8**	**26.2**	**23.7**	**22.2**
Esters	1.2	2.9	3.5	8.3	15.0	18.8	14.4	10.9	13.0
Ethers	-	-	-	2.5	-	-	2.5	-	-
Ketones	30.5	37.7	16.7	20.9	11.5	8.8	10.6	8.6	6.1
Aldehydes	-	1.0	-	-	0.8	-	-	0.9	1.0
Acids	2.1	4.5	7.8	4.4	0.9	3.8	3.6	3.3	6.9
Alcohols	2.1	0.5	-	0.8	1.5	9.3	1.5	3.0	6.6
Furans	1.0	10.6	10.4	-	-	-	-	-	0.5
Total Oxygenated	**37.0**	**57.2**	**38.4**	**36.9**	**29.7**	**40.6**	**32.6**	**26.7**	**34.0**
1,4:3,6-Dianhydro-α-D-glucopyranose	1.2	1.9	-	-	-	-	-	-	-
2,3,4-Trimethyllevoglucosan	0.5	0.4	-	-	-	-	-	-	-
Maltol	-	0.7	0.7	-	-	-	-	-	-
Others	0.4	1.5	-	-	-	-	-	-	-
Total Anhydrosugars	**2.1**	**4.5**	**0.7**	-	-	-	-	-	-
Phenols	8.6	1.0	2.7	11.3	9.3	4.7	8.9	10.2	6.0
***p*-Cresol**	-	-	-	4.1	5.3	1.4	4.8	6.2	4.2
Total Phenolics	**8.6**	**1.0**	**2.7**	**15.4**	**14.6**	**6.1**	**13.7**	**16.4**	**10.2**
Olefin	-	0.3	1.0	1.9	2.1	2.1	2.9	2.3	1.8
Paraffin	-	1.2	0.8	6.2	7.7	8.1	11.6	10.4	5.2
BTXS[a]	-	0.6	1.2	12.4	20.6	25.0	13.1	18.6	20.9
Polyaromatic	-	-	-	-	0.4	0.3	-	0.8	2.8
Total Hydrocarbons	-	**2.1**	**3.0**	**20.5**	**30.8**	**35.5**	**27.6**	**32.1**	**30.7**
Total S-containing compounds	**-**	**1.0**	**1.5**	**-**	**2.0**	**2.7**	**-**	**0.9**	**3.0**

[a] BTXS- Benzene, Toluene, Xylene, and Styrene

samples. However, inherent minerals in RB and residual acid in TB_nw facilitated denitrogenation reactions to generate more volatile-N compounds than TB. For instance, at 300 ℃, total N-compounds were 53% for RB and TB_nw and 34% for TB. Significant thermal cracking of heavy *N*-heterocyclic compounds to simple aromatic/aliphatic N-compounds occurred at higher pyrolysis temperatures (500–700 ℃), reducing total nitrogenated compounds in the bio-oil to ≈ 23% for all samples. The effect of pre-treatment on the evolution of N-compounds was less intense at 500 and 700 ℃. It has been observed that the interaction between mineral matter and N-containing compounds in biosolids was strongly limited by pyrolysis temperature [52].

Notably, anhydrosugars (including sugar alcohols) production was sensitive to pyrolysis temperatures. It was detected only at 300 ℃, and the yield was improved by more than 50% following the removal of AAEMs in TB. At 500–700 ℃, pre-treatment had no impact on the production of anhydrosugars as they are highly susceptible to secondary degradation facilitated by metal and acid catalysts as well as higher pyrolysis temperatures [53]. However, biosolids pre-treatment favoured the production of sugar dehydration products such as maltol and furans (10%), mainly comprising 3-HMF, furfural, and 5-methyl furfural. The acid catalysis of sugars is a popular route to enhance the formation of furfural compounds [54]. The passivation of AAEMs by acid infusion selectively enhanced sugar dehydration products, such as levoglucosenone and furfural, whose yield was observed to be related to the quantity of acid added [55]. Phenols and their derivatives may originate from biosolids pyrolysis through the secondary decomposition of polysaccharides and proteins and are generally enhanced at higher temperatures from aromatisation reactions [56]. At 300 ℃, the total phenolics yield was less than 10%, mostly detected in RB bio-oil. At higher temperatures, phenolics yield increased to ≈ 15% for both RB and TB, whereas it was no more than 10% for TB_nw. Mineral removal by pre-treatment had no significant effect on phenol production; however, residual acid in TB_nw suppressed phenol formation relative to RB. Other works [36,57] have also suggested that phenol precursor such as lignin is relatively inert to AAEMs. While AAEMs are largely inert in catalysing the cleavage of the ester group in lignin to produce guaiacols (vinyl-phenols), it has been found effective in promoting the cleavage of β-O-4 aryl ether bonds to produce simple phenolic monomers such as cresols [55]. This could explain the higher yield of *p*-cresol with acid-pre-treated biosolids compared to RB.

Hydrocarbon production increased monotonically with temperature, and it grew from 0% to 3% at 300 ℃ to 20–35% at 500 ℃ for all samples, with RB having the lowest yield. Raising the temperature to 700 ℃ increased hydrocarbon yield to 28% for RB, slightly decreasing the yield to about 32% for treated biosolids. Monoaromatic hydrocarbons, mainly benzene, toluene, xylene, and styrene (BTXS), are the major compounds in the bio-oil at higher temperatures ≥ 500 ℃. In contrast, aliphatic hydrocarbons, mainly paraffin and olefin, were detected in bio-oil from untreated biosolids at < 500 ℃. Acid pre-treatment enhanced aromatisation reactions, which increased the yields of monoaromatic hydrocarbons due to the suppression of AAEMs-catalysed ring opening and fragmentation reactions that would otherwise convert -CH to light oxygenates, COx gases, and char [36,58]. In a previous study [36], acid washing and infusion enhanced the formation of aromatic hydrocarbons by ~30%; however, both pre-treatment did not significantly change the yield of olefins, similar to the observation in the current work. The weaker effect of inherent AAEMs caused by acid pre-treatment increased the formation of undesired stable polycyclic aromatic hydrocarbons (PAHs) in bio-oil from TB and TB_nw; however, PAHs were not detected in RB bio-oil at all temperatures. AAEMs and their minerals can enhance the cracking of heavy PAHs into monoaromatics, particularly at higher temperatures [59]. Lastly, aromatic sulfur compounds such as benzisothiazole, thiazolidine, thiophene, and aliphatic S-compounds, mainly methyl sulfides, were detected in the bio-oil obtained from treated

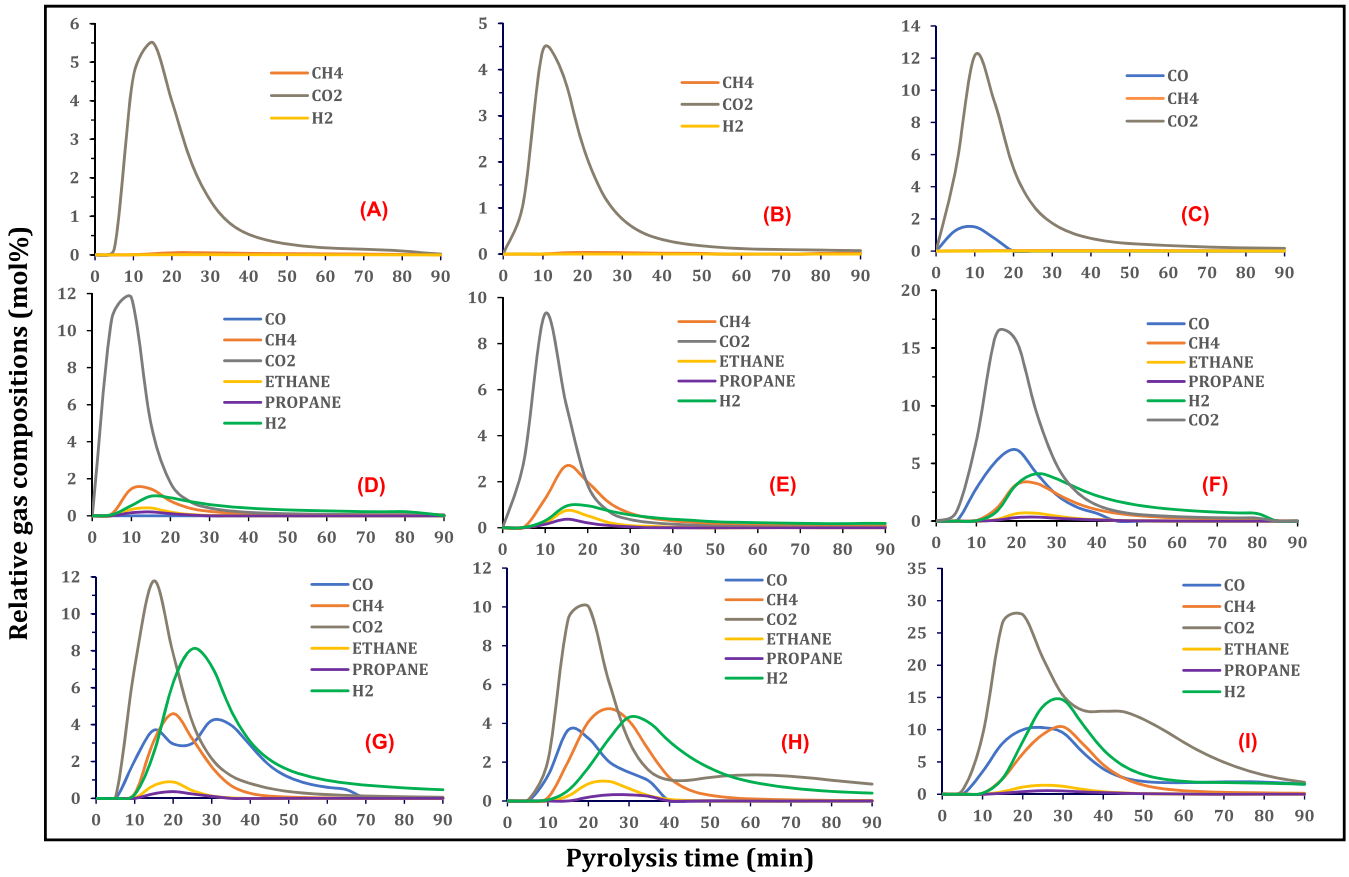

Fig. 5. Effect of pre-treatment and temperature on pyrolysis gas compositions (A) RB300 (B) TB300 (C)TB_nw300 (D) RB500 (E) TB500 (F) TB_nw500 (G) RB700 (H) TB700 (I) TB_nw700.

biosolids. The evolution of these S-compounds was stronger at ≥ 500 ℃ and for TB_nw (up to 3%). Therefore, the acid treatment should be accompanied by a neutralisation step, as in TB, to mitigate the release of volatile S-compounds.

Due to the generally high nitrogen and oxygen contents, the bio-oil may not be suitable as fuel for energy recovery. However, the chemical value of the bio-oil obtained at 300 ℃ can be explored for the selective recovery of *N*-containing compounds, and the ketone-rich fraction can be subjected to catalytic hydrodeoxygenation to produce olefins [60]. Therefore, biosolids pyrolysis at 300 ℃ may be considered a thermal pre-treatment step for the reduction of nitrogen and oxygen contents and improve hydrocarbon yield during subsequent pyrolysis at higher temperatures [61]. The addition of acid pre-treatment can further enhance the chemical value of the bio-oil by increasing sugars, furans, and aromatic hydrocarbon, as observed in the current work. Fonts et al. [62] reported that ammonia, α-olefins, n-paraffins, aromatic hydrocarbons, nitriles, phenols, fatty acids, short carboxylic acids and indole were the most attractive chemical compounds in biosolids bio-oil.

3.6. *Effect of pre-treatment on pyrolysis gas compositions*

The evolution profile of non-condensable gases from the pyrolysis of raw and treated biosolids at 300–700 ℃ is shown in Fig. 5. The identified gas components are carbon oxides (CO and CO_2), H_2, and C_1-C_3 saturated hydrocarbon gases (methane, ethane, and propane). The concentration of the gases was low at the start of pyrolysis as the feed was gradually heated to the desired temperature. The gas concentration steadily increased between 10 and 30 min; after that, the concentration gradually decreased, reaching zero at 60–90 min. The most abundant gas components were H_2, CO, CO_2 and CH_4, while only traces of ethane and propane were detected at higher pyrolysis temperatures > 500 ℃. Generally, gas production increased with increasing pyrolysis temperature due to the profound thermal cracking of primary decomposition products and secondary reactions. At 300 ℃ (Fig. 5(A-C)), CO_2 was the dominant gas component, with traces of CH_4 and H_2 in the pyrolysis gas stream largely from the decarboxylation of organic matter. At higher pyrolysis temperatures, gasification reactions matured, and more gas components were formed at higher concentrations stemming from the thermal cracking of heavy molecular weight volatiles to lighter ones accompanied by the release of C_1-C_3 hydrocarbons (Fig. 5(D-I)). At 700 ℃ (Fig. 5(G-I)), the gas evolution was stronger, and the concentrations were highest attributed to the profound secondary cracking reactions heightened by char-volatile interactions [63].

The removal or passivation of inherent metals in biosolids via pre-treatment affected the gas evolution and concentration during pyrolysis, especially at higher pyrolysis temperatures. The pyrolysis of TB produced less CO_2, CO, and H_2 but slightly more C_1-C_3 hydrocarbons than RB, suggesting that pre-treatment inhibited gas production due to the inferior catalytic cracking effect of ash elements. For example, at 700 ℃, the highest CO and H_2 concentration was 4.2 mol% and 8 mol%, respectively, for RB (Fig. 5(G)), and it was 3.6 mol% and 4.3 mol%, respectively, for TB (Fig. 5(H)). Secondary cracking was prominent and catalysed by the native metal in RB, leading to higher concentrations of CO and H_2. The second CO peak in RB at 700 ℃ (Fig. 5(G)) after 30 min pyrolysis time can be attributed to Boudouard char gasification reactions where CO_2 is reacted with carbon to give CO [30]. Notably, the highest gas concentrations were observed during the pyrolysis of TB_nw at all temperatures. The XRD pattern of TB_nw identified $Ca(HSO_4)_2$ and

$Fe(HSO_4)_3$ as the major acidic sulfate salts, which facilitated H_2 production via the release of H^+ through thermal hydrolysis reactions to form normal sulfate salts ($CaSO_4$ and $Fe_2(SO_4)_3$) [64]. The presence of residual acid in TB_nw had a remarkable catalytic effect on gas production, with CO_2, CO, CH_4, and H_2 yield reaching a maximum concentration of 28 mol%, 10 mol%, 10.5 mol%, and 15 mol%, respectively (Fig. 5(I)). Whereas, with the full spectrum of metals in RB, the maximum gas concentration at 700 ℃ was 12 mol% CO_2, 4 mol% CO, 4.5 mol% CH_4, and 8 mol% H_2 (Fig. 5(G)). The improved gas production in TB_nw despite lean mineral matter compared to RB was attributed to the dehydration reactions catalysed by residual H_2SO_4, favouring water-gas reactions [42]. Biosolids acid pre-treatment for demineralisation (as in TB) can be helpful to weaken gas production and CO_2 release, while pre-treatment as in TB_nw strengthened gas production, and CO_2 yield was more than 2-fold higher than that from RB.

4. Conclusions

The quality of biosolids as feedstock for pyrolysis can be improved by acid pre-treatment to selectively remove the ash-forming elements and HMs without degrading the organic matter. Mild acid pre-treatment process (using 3% v/v H_2SO_4 at 25 ℃ for 60 min) followed by a water washing step achieved about 40% reduction of ash content and a 10% increase in volatile matter with carbon retention of 80%. In contrast, the acid treatment without the water washing step achieved lower demineralisation efficiency (28%) with higher carbon retention (88%). At all operating temperatures, the pyrolysis of neutralised acid-treated biosolids produced higher bio-oil and lower biochar yield due to improved organic matter devolatilisation and inorganic content reduction. The presence of residual acid in treated biosolids inhibited organic matter conversion to bio-oil; however, it enhanced gas production attributed to dehydration reactions and hydrolysis of acidic metal sulfate salts to normal metal sulfate salts. Biochar obtained from treated biosolids had higher organic matter retention, calorific value, fuel ratio, and fixed carbon due to the weakened catalytic cracking of organics, particularly at higher pyrolysis temperatures. Biosolids pre-treatment increased the stability and reduced the concentration and bioavailability of HMs in the derived biochar. The bio-oil composition was impacted by pre-treatment, and at 300 ℃, anhydrosugars yield doubled in treated biosolids' bio-oil compared to raw biosolids' bio-oil. While pre-treatment did not have much effect on phenol production, monoaromatic hydrocarbon yield was remarkably improved. However, the evolution of PAHs and sulfur-containing compounds was stronger during the pyrolysis of treated biosolids than raw biosolids. Biosolids acid pre-treatment with the water washing step is preferred to increase bio-oil yield and enhance biochar quality.

CRediT authorship contribution statement

Ibrahim Gbolahan Hakeem: Conceptualization, Methodology, Formal analysis, Investigation, Writing - original draft, Writing - review & editing. **Pobitra Halder:** Validation, Writing – review & editing. **Savankumar Patel:** Writing – review & editing. **Abhishek Sharma:** Writing – review & editing. **Rajender Gupta:** Writing – review & editing. **Aravind Surapaneni:** Resources, Supervision. **Jorge Paz-Ferreiro:** Supervision, Writing – review & editing. **Kalpit Shah:** Conceptualization, Methodology, Validation, Supervision, Project administration.

Declaration of Competing Interest

The authors declare that they have no known competing financial interests or personal relationships that could have appeared to influence the work reported in this paper.

Data availability

Data will be made available on request.

Acknowledgements

This work is supported through Top-Up Scholarships provided by the School of Engineering, RMIT University and the ARC Training Centre for the Transformation of Australia's Biosolids Resource at RMIT University, Australia. The use of the Scanning Electron Microscope instrument in the RMIT Microanalysis and Microscopy Facility is acknowledged. The BET equipment in the Advanced Porous Materials Lab at RMIT University was used in this study. Finally, the first author acknowledged the PhD research stipend scholarship received from RMIT University, Australia.

Appendix A. Supporting information

Supplementary data associated with this article can be found in the online version at doi:10.1016/j.jaap.2023.106087.

References

[1] A. Gianico, C.M. Braguglia, A. Gallipoli, D. Montecchio, G. Mininni, Land application of biosolids in Europe: possibilities, con-straints and future perspectives, Water 13 (2021) 103, https://doi.org/10.3390/W13010103.
[2] N. Gao, K. Kamran, C. Quan, P.T. Williams, Thermochemical conversion of sewage sludge: A critical review, Prog. Energy Combust. Sci. 79 (2020), 100843, https://doi.org/10.1016/j.pecs.2020.100843.
[3] W. Zhang, Y. Liang, Effects of hydrothermal treatments on destruction of per- and polyfluoroalkyl substances in sewage sludge, Environ. Pollut. 285 (2021), 117276, https://doi.org/10.1016/J.ENVPOL.2021.117276.
[4] J.J. Ross, D.H. Zitomer, T.R. Miller, C.A. Weirich, P.J. Mcnamara, Emerging investigators series: pyrolysis removes common microconstituents triclocarban, triclosan, and nonylphenol from biosolids, Environ. Sci. Water Res. Technol. 2 (2016) 282–289, https://doi.org/10.1039/C5EW00229J.
[5] O.S. Djandja, Z.C. Wang, F. Wang, Y.P. Xu, P.G. Duan, Pyrolysis of municipal sewage sludge for biofuel production: A review, Ind. Eng. Chem. Res. 59 (2020) 16939–16956, https://doi.org/10.1021/acs.iecr.0c01546.
[6] S. Patel, S. Kundu, P. Halder, N. Ratnnayake, M.H. Marzbali, S. Aktar, E. Selezneva, J. Paz-Ferreiro, A. Surapaneni, C.C. de Figueiredo, A. Sharma, M. Megharaj, K. Shah, A critical literature review on biosolids to biochar: an alternative biosolids management option, Rev. Environ. Sci. Biotechnol. 19 (2020) 807–841, https://doi.org/10.1007/s11157-020-09553-x.
[7] P. Giudicianni, V. Gargiulo, C.M. Grottola, M. Alfè, A.I. Ferreiro, M.A.A. Mendes, M. Fagnano, R. Ragucci, Inherent metal elements in biomass pyrolysis: a review, Energy Fuels 35 (2021) 5407–5478, https://doi.org/10.1021/ACS.ENERGYFUELS.0C04046.
[8] H. Nan, F. Yang, L. Zhao, O. Mašek, X. Cao, Z. Xiao, Interaction of inherent minerals with carbon during biomass pyrolysis weakens biochar carbon sequestration potential, ACS Sustain. Chem. Eng. 7 (2018) 1591–1599, https://doi.org/10.1021/ACSSUSCHEMENG.8B05364.
[9] Y. Niu, H. Tan, S. Hui, Ash-related issues during biomass combustion: Alkali-induced slagging, silicate melt-induced slagging (ash fusion), agglomeration, corrosion, ash utilization, and related countermeasures, Prog. Energy Combust. Sci. 52 (2016) 1–61, https://doi.org/10.1016/j.pecs.2015.09.003.
[10] M.J. Bentley, J.P. Kearns, B.M. Murphy, R.S. Summers, Pre-pyrolysis metal and base addition catalyzes pore development and improves organic micropollutant adsorption to pine biochar, Chemosphere 286 (2022), 131949, https://doi.org/10.1016/J.CHEMOSPHERE.2021.131949.
[11] I.G. Hakeem, P. Halder, C.C. Dike, K. Chiang, A. Sharma, J. Paz-Ferreiro, K. Shah, Advances in biosolids pyrolysis: Roles of pre-treatments, catalysts, and co-feeding on products distribution and high-value chemical production, J. Anal. Appl. Pyrolysis 166 (2022), 105608, https://doi.org/10.1016/J.JAAP.2022.105608.
[12] R. Patel, P. Zaveri, N.S. Munshi, Microbial fuel cell, the Indian scenario: developments and scopes, Biofuels 10 (2019) 101–108, https://doi.org/10.1080/17597269.2017.1398953.
[13] N.A. Haji Morni, C.M. Yeung, H. Tian, Y. Yang, N. Phusunti, M.S. Abu Bakar, A. K. Azad, Catalytic fast Co-Pyrolysis of sewage sludge−sawdust using mixed metal oxides modified with ZSM-5 catalysts on dual-catalysts for product upgrading, J. Energy Inst. 94 (2021) 387–397, https://doi.org/10.1016/J.JOEI.2020.10.005.
[14] Z. Qiu, Y. Zhai, S. Li, X. Liu, X. Liu, B. Wang, Y. Liu, C. Li, Y. Hu, Catalytic co-pyrolysis of sewage sludge and rice husk over biochar catalyst: Bio-oil upgrading and catalytic mechanism, Waste Manag 114 (2020) 225–233, https://doi.org/10.1016/J.WASMAN.2020.07.013.
[15] N. Rathnayake, S. Patel, I.G. Hakeem, J. Pazferreiro, A. Sharma, R. Gupta, C. Rees, D. Bergmann, J. Blackbeard, A. Surapaneni, K. Shah, Co-pyrolysis of biosolids with lignocellulosic biomass: Effect of feedstock on product yield and composition, Process Saf. Environ. Prot. (2023), https://doi.org/10.1016/J.PSEP.2023.02.087.

[16] X. Wang, S. Deng, H. Tan, A. Adeosun, M. Vujanović, F. Yang, N. Duić, Synergetic effect of sewage sludge and biomass co-pyrolysis: A combined study in thermogravimetric analyzer and a fixed bed reactor, Energy Convers. Manag 118 (2016) 399–405, https://doi.org/10.1016/j.enconman.2016.04.014.
[17] I.G. Hakeem, P. Halder, M.H. Marzbali, S. Patel, N. Rathnayake, A. Surapaneni, G. Short, J. Paz-Ferreiro, K. Shah, Mild sulphuric acid pre-treatment for metals removal from biosolids and the fate of metals in the treated biosolids derived biochar, J. Environ. Chem. Eng. 10 (2022), 107378, https://doi.org/10.1016/J.JECE.2022.107378.
[18] G. Liu, M.M. Wright, Q. Zhao, R.C. Brown, Hydrocarbon and ammonia production from catalytic pyrolysis of sewage sludge with acid pretreatment, ACS Sustain. Chem. Eng. 4 (2016) 1819–1826, https://doi.org/10.1021/acssuschemeng.6b00016.
[19] S. Tang, C. Zheng, Z. Zhang, Effect of inherent minerals on sewage sludge pyrolysis: Product characteristics, kinetics and thermodynamics, Waste Manag 80 (2018) 175–185, https://doi.org/10.1016/j.wasman.2018.09.012.
[20] Z. Yang, D. Wang, G. Wang, S. Zhang, Z. Cheng, J. Xian, Y. Pu, T. Li, Y. Jia, Y. Li, W. Zhou, X. Xu, Removal of Pb, Zn, Ni and Cr from industrial sludge by biodegradable washing agents: Caboxyethylthiosuccinic acid and itaconic-acrylic acid, J. Environ. Chem. Eng. 9 (2021), 105846, https://doi.org/10.1016/J.JECE.2021.105846.
[21] R. Kumar, V. Strezov, H. Weldekidan, J. He, S. Singh, T. Kan, B. Dastjerdi, Lignocellulose biomass pyrolysis for bio-oil production: A review of biomass pre-treatment methods for production of drop-in fuels, Renew. Sustain. Energy Rev. 123 (2020), 109763, https://doi.org/10.1016/J.RSER.2020.109763.
[22] V.T. Pham, C.Y. Guan, P.C. Han, B.M. Matsagar, K.C.W. Wu, T. Ahamad, C. Y. Chang, C.P. Yu, Acid-catalyzed hydrothermal treatment of sewage sludge: effects of reaction temperature and acid concentration on the production of hydrolysis by-products, Biomass-.-. Convers. Biorefinery. 13 (2021) 7533–7546, https://doi.org/10.1007/S13399-021-01495-W/FIGURES/5.
[23] I.G. Hakeem, P. Halder, S. Aktar, M.H. Marzbali, A. Sharma, A. Surapaneni, G. Short, J. Paz-Ferreiro, K. Shah, Investigations into the closed-loop hydrometallurgical process for heavy metals removal and recovery from biosolids via mild acid pre-treatment, Hydrometallurgy 218 (2023), 106044, https://doi.org/10.1016/J.HYDROMET.2023.106044.
[24] I. Beauchesne, R. Ben Cheikh, G. Mercier, J.F. Blais, T. Ouarda, Chemical treatment of sludge: In-depth study on toxic metal removal efficiency, dewatering ability and fertilizing property preservation, Water Res 41 (2007) 2028–2038, https://doi.org/10.1016/J.WATRES.2007.01.051.
[25] J. Shao, R. Yan, H. Chen, H. Yang, D.H. Lee, Catalytic effect of metal oxides on pyrolysis of sewage sludge, Fuel Process. Technol. 91 (2010) 1113–1118, https://doi.org/10.1016/j.fuproc.2010.03.023.
[26] S. Tang, C. Zheng, F. Yan, N. Shao, Y. Tang, Z. Zhang, Product characteristics and kinetics of sewage sludge pyrolysis driven by alkaline earth metals, energy 153 (2018) 921–932, https://doi.org/10.1016/j.energy.2018.04.108.
[27] S. Tang, S. Tian, C. Zheng, Z. Zhang, Effect of Calcium Hydroxide on the Pyrolysis Behavior of Sewage Sludge: Reaction Characteristics and Kinetics, Energy Fuels 31 (2017) 5079–5087, https://doi.org/10.1021/acs.energyfuels.6b03256.
[28] Y. Kim, W. Parker, A technical and economic evaluation of the pyrolysis of sewage sludge for the production of bio-oil, Bioresour. Technol. 99 (2008) 1409–1416, https://doi.org/10.1016/j.biortech.2007.01.056.
[29] N. Rathnayake, S. Patel, P. Halder, S. Aktar, J. Pazferreiro, A. Sharma, A. Surapaneni, K. Shah, Co-pyrolysis of biosolids with alum sludge: Effect of temperature and mixing ratio on product properties, J. Anal. Appl. Pyrolysis 163 (2022), 105488, https://doi.org/10.1016/J.JAAP.2022.105488.
[30] S. Patel, S. Kundu, P. Halder, G. Veluswamy, B. Pramanik, Slow pyrolysis of biosolids in a bubbling fluidised bed reactor using biochar, activated char and lime, J. Anal. Appl. Pyrolysis 144 (2019) 1–11, https://doi.org/10.1016/j.jaap.2019.104697.
[31] S.A. Channiwala, P.P. Parikh, A unified correlation for estimating HHV of solid, liquid and gaseous fuels, Fuel 81 (2002) 1051–1063, https://doi.org/10.1016/S0016-2361(01)00131-4.
[32] W.L. Lindsay, W.A. Norvell, Development of a DTPA Soil Test for Zinc, Iron, Manganese, and Copper, Soil Sci. Soc. Am. J. 42 (1978) 421–428, https://doi.org/10.2136/SSSAJ1978.03615995004200030009X.
[33] E.P.A. Victoria, Guidelines for Environmental Mangement: Biosolids Land Application, Southbank, Victoria 3006, Australia, 2004.
[34] X. Wang, L. Sheng, X. Yang, Pyrolysis characteristics and pathways of protein, lipid and carbohydrate isolated from microalgae Nannochloropsis sp, Bioresour. Technol. 229 (2017) 119–125, https://doi.org/10.1016/J.BIORTECH.2017.01.018.
[35] S.R. Patel, S.K. Kundu, P.K. Halder, A. Setiawan, J. Paz-Ferreiro, A. Surapaneni, K. V. Shah, A Hybrid Kinetic Analysis of the Biosolids Pyrolysis using Thermogravimetric Analyser, ChemistrySelect 3 (2018) 13400–13407, https://doi.org/10.1002/slct.201802957.
[36] K. Wang, J. Zhang, B.H. Shanks, R.C. Brown, The deleterious effect of inorganic salts on hydrocarbon yields from catalytic pyrolysis of lignocellulosic biomass and its mitigation, Appl. Energy 148 (2015) 115–120, https://doi.org/10.1016/j.apenergy.2015.03.034.
[37] X. Zhu, L. Zhao, F. Fu, Z. Yang, F. Li, W. Yuan, M. Zhou, W. Fang, G. Zhen, X. Lu, X. Zhang, Pyrolysis of pre-dried dewatered sewage sludge under different heating rates: Characteristics and kinetics study, Fuel 255 (2019), 115591, https://doi.org/10.1016/J.FUEL.2019.05.174.
[38] N. Gao, J. Li, B. Qi, A. Li, Y. Duan, Z. Wang, Thermal analysis and products distribution of dried sewage sludge pyrolysis, J. Anal. Appl. Pyrolysis 105 (2014) 43–48, https://doi.org/10.1016/J.JAAP.2013.10.002.
[39] S. Zhou, Z. Wang, S. Liaw, C. Li, M. Garcia-perez, Effect of sulfuric acid on the pyrolysis of Douglas fir and hybrid poplar wood: Py-GC / MS and TG studies, J. Anal. Appl. Pyrolysis 104 (2013) 117–130, https://doi.org/10.1016/j.jaap.2013.08.013.
[40] S. Aktar, M.A. Hossain, N. Rathnayake, S. Patel, G. Gasco, A. Mendez, C. de Figueiredo, A. Surapaneni, K. Shah, J. Paz-Ferreiro, Effects of temperature and carrier gas on physico-chemical properties of biochar derived from biosolids, J. Anal. Appl. Pyrolysis 164 (2022), 105542, https://doi.org/10.1016/J.JAAP.2022.105542.
[41] D. Carpenter, T.L. Westover, S. Czernik, W. Jablonski, Biomass feedstocks for renewable fuel production: a review of the impacts of feedstock and pretreatment on the yield and product distribution of fast pyrolysis bio-oils and vapors, Green. Chem. 16 (2014) 384–406, https://doi.org/10.1039/C3GC41631C.
[42] S. Zhou, D. Mourant, C. Lievens, Y. Wang, C. Li, M. Garcia-perez, Effect of sulfuric acid concentration on the yield and properties of the bio-oils obtained from the auger and fast pyrolysis of Douglas Fir, Fuel 104 (2013) 536–546, https://doi.org/10.1016/j.fuel.2012.06.010.
[43] Y. Zhang, P. Lv, J. Wang, J. Wei, P. Cao, N. Bie, Y. Bai, G. Yu, Product characteristics of rice straw pyrolysis at different temperature: Role of inherent alkali and alkaline earth metals with different occurrence forms, J. Energy Inst. 101 (2022) 201–208, https://doi.org/10.1016/J.JOEI.2022.01.016.
[44] X. Sun, R. Shan, X. Li, J. Pan, X. Liu, R. Deng, J. Song, Characterization of 60 types of Chinese biomass waste and resultant biochars in terms of their candidacy for soil application, GCB Bioenergy 9 (2017) 1423–1435, https://doi.org/10.1111/GCBB.12435.
[45] X. Xiao, Z. Chen, B. Chen, H/C atomic ratio as a smart linkage between pyrolytic temperatures, aromatic clusters and sorption properties of biochars derived from diverse precursory materials, Sci. Rep. 6 (2016), https://doi.org/10.1038/srep22644.
[46] M. Praspaliauskas, N. Pedišius, N. Striuigas, Elemental Migration and Transformation from Sewage Sludge to Residual Products during the Pyrolysis Process, Energy Fuels 32 (2018) 5199–5208, https://doi.org/10.1021/ACS.ENERGYFUELS.8B00196/ASSET/IMAGES/LARGE/EF-2018-001968_0006.JPEG.
[47] Z. Zhang, R. Ju, H. Zhou, H. Chen, Migration characteristics of heavy metals during sludge pyrolysis, Waste Manag 120 (2021) 25–32, https://doi.org/10.1016/j.wasman.2020.11.018.
[48] D. del Mundo Dacera, S. Babel, Use of citric acid for heavy metals extraction from contaminated sewage sludge for land application, Water Sci. Technol. 54 (2006) 129–135, https://doi.org/10.2166/wst.2006.764.
[49] Z. Cui, G. Xu, B. Ormeci, H. Liu, Z. Zhang, Transformation and stabilization of heavy metals during pyrolysis of organic and inorganic-dominated sewage sludges and their mechanisms, Waste Manag 150 (2022) 57–65, https://doi.org/10.1016/J.WASMAN.2022.06.023.
[50] A. Fullana, J.A. Conesa, R. Font, I. Martın-Gullon, Pyrolysis of sewage sludge: nitrogenated compounds and pretreatment effects, J. Anal. Appl. Pyrolysis 69 (2003) 561–575, https://doi.org/10.1016/S0165-2370(03)00052-4.
[51] X. Yang, B. Wang, Y. Guo, F. Yang, F. Cheng, Co-hydrothermal carbonization of sewage sludge and coal slime for clean solid fuel production: a comprehensive assessment of hydrochar fuel characteristics and combustion behavior, Biomass-.-. Convers. Biorefinery (2022), https://doi.org/10.1007/s13399-022-03601-y.
[52] L.H. Wei, L.N. Wen, M.J. Liu, T.H. Yang, Interaction Characteristics of Mineral Matter and Nitrogen during Sewage Sludge Pyrolysis, Energy Fuels 30 (2016) 10505–10510, https://doi.org/10.1021/acs.energyfuels.6b02146.
[53] I.G. Hakeem, P. Halder, M.H. Marzbali, S. Patel, S. Kundu, J. Paz-Ferreiro, A. Surapaneni, K. Shah, Research progress on levoglucosan production via pyrolysis of lignocellulosic biomass and its effective recovery from bio-oil, J. Environ. Chem. Eng. 9 (2021), 105614, https://doi.org/10.1016/j.jece.2021.105614.
[54] S.R.G. Oudenhoven, R.J.M. Westerhof, N. Aldenkamp, D.W.F. Brilman, S.R. A. Kersten, Demineralization of wood using wood-derived acid: Towards a selective pyrolysis process for fuel and chemicals production, J. Anal. Appl. Pyrolysis 103 (2013) 112–118, https://doi.org/10.1016/j.jaap.2012.10.002.
[55] S. Zhou, Y. Xue, J. Cai, C. Cui, Z. Ni, Z. Zhou, An understanding for improved biomass pyrolysis: Toward a systematic comparison of different acid pretreatments, Chem. Eng. J. 411 (2021), 128513, https://doi.org/10.1016/J.CEJ.2021.128513.
[56] X. Huang, J.P. Cao, P. Shi, X.Y. Zhao, X.B. Feng, Y.P. Zhao, X. Fan, X.Y. Wei, T. Takarada, Influences of pyrolysis conditions in the production and chemical composition of the bio-oils from fast pyrolysis of sewage sludge, J. Anal. Appl. Pyrolysis 110 (2014) 353–362, https://doi.org/10.1016/J.JAAP.2014.10.003.
[57] P.R. Patwardhan, R.C. Brown, B.H. Shanks, Understanding the Fast Pyrolysis of Lignin, ChemSusChem 4 (2011) 1629–1636, https://doi.org/10.1002/CSSC.201100133.
[58] D.L. Dalluge, T. Daugaard, P. Johnston, N. Kuzhiyil, M.M. Wright, R.C. Brown, Continuous production of sugars from pyrolysis of acid-infused lignocellulosic biomass, Green. Chem. 16 (2014) 4144–4155, https://doi.org/10.1039/c4gc00602j.
[59] S. Hu, L. Jiang, Y. Wang, S. Su, L. Sun, B. Xu, L. He, J. Xiang, Effects of inherent alkali and alkaline earth metallic species on biomass pyrolysis at different temperatures, Bioresour. Technol. 192 (2015) 23–30, https://doi.org/10.1016/j.biortech.2015.05.042.
[60] A. Witsuthammakul, T. Sooknoi, Selective hydrodeoxygenation of bio-oil derived products: ketones to olefins, Catal. Sci. Technol. 5 (2015) 3639–3648, https://doi.org/10.1039/C5CY00367A.
[61] Y. Liu, Y. Zhai, S. Li, X. Liu, X. Liu, B. Wang, Z. Qiu, C. Li, Production of bio-oil with low oxygen and nitrogen contents by combined hydrothermal pretreatment and

pyrolysis of sewage sludge, energy 203 (2020), 117829, https://doi.org/10.1016/J.ENERGY.2020.117829.

[62] I. Fonts, A. Navarro-Puyuelo, N. Ruiz-Gómez, M. Atienza-Martínez, A. Wisniewski, G. Gea, Assessment of the production of value-added chemical compounds from sewage sludge pyrolysis liquids, Energy Technol. 5 (2017) 151–171, https://doi.org/10.1002/ente.201600183.

[63] Q. Guo, Z. Cheng, G. Chen, B. Yan, J. Li, L. Hou, F. Ronsse, Assessment of biomass demineralization on gasification: From experimental investigation, mechanism to potential application, Sci. Total Environ. 726 (2020), 138634, https://doi.org/10.1016/J.SCITOTENV.2020.138634.

[64] N. Kuzhiyil, D. Dalluge, X. Bai, H. Kim, Pyrolytic sugars from cellulosic biomass, ChemSusChem 0 (2012) 1–10, https://doi.org/10.1002/cssc.201200341.